Multi-modal Approach to Modeling Creep Deformation In Ni-Base Superalloys

Program No. FE0031554

Federal Project Manager: Richard Dunst
Technology Manager :Briggs White

Ridwan Sakidja[1], Wai-Yim Ching[2] and Caizhi Zhou[3]

[1] Dept. of Physics, Astronomy & Materials Science, Missouri State University

[2] Dept. of Physics & Astronomy, Univ. of Missouri-Kansas City

[3] Dept. of Mat. Sci & Engr., Missouri University of Science & Technology at Rolla

2019 Annual Review Meeting for Crosscutting Research,

April 9-11, 2019, Pittsburgh, PA 15219

Motivations

- Developing next generation high strength materials.
- Major difficulties: predicting the mechanical failures initiated from atomistic-based models
- Reducing level of uncertainty for creep failure during tertiary creep stage.
- *Nickel based superalloys*:

  ➔ FCC (γ) + Ni_3Al(γ') (+ carbide prep).– model system

  ➔ Haynes 282 & Inconel 740/740H - targets
- Multi modal approaches are needed.

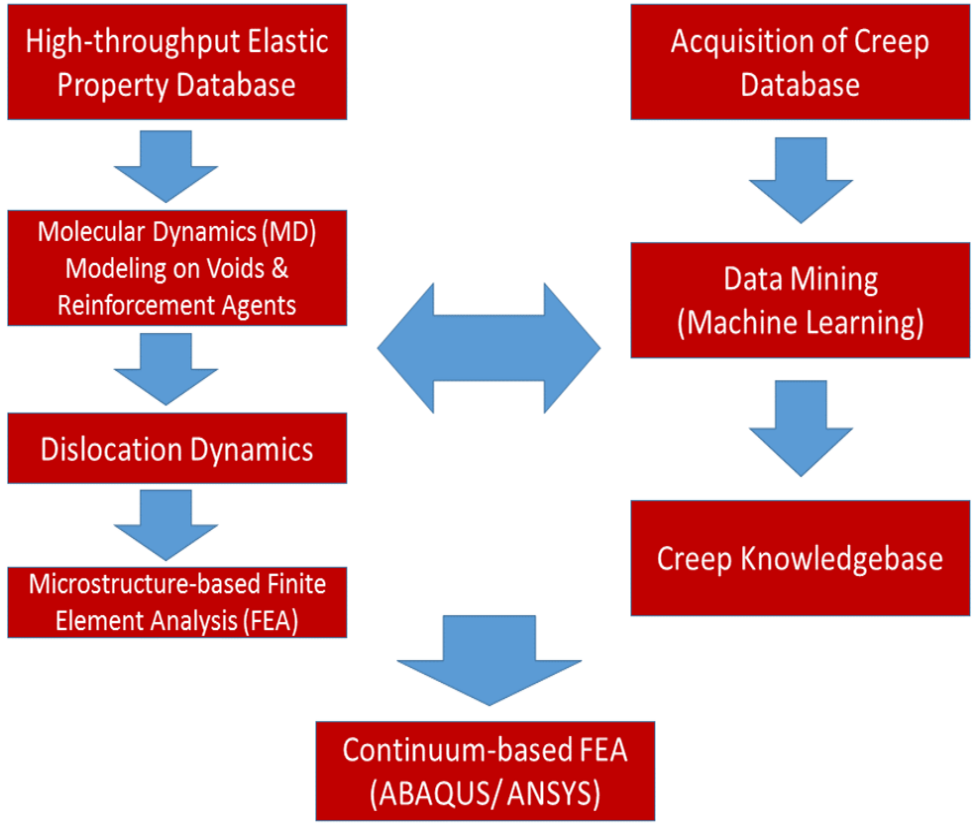

Failure in polycrystalline Ni-based superalloys

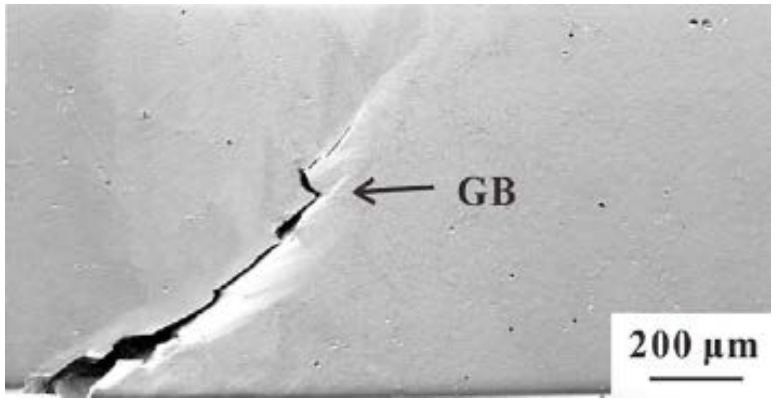

Adv. Eng. Mater. 2019, 21: 1800856

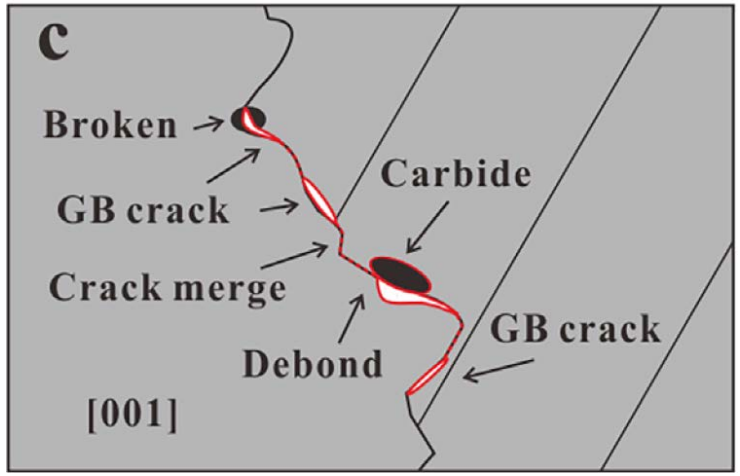

Experiment results show: Voids/cracks always nucleated from the grain boundaries (GBs) in polycrystalline Ni-based superalloys.

Ultimate goal of this work:

Understand how the GBs affect the void growth in polycrystalline Ni-based superalloys by using a full field crystal plasticity finite element model (CPFEM) to provide design guideline for processing Ni-based superalloys with desired mechanical properties.

Modeling Approaches

1. Electronic Structure Calculation Approach

- **Vienna *ab-initio* simulation package (VASP) [1]:**
  - Efficient for structural relaxation, force and stress relation calculation.
- **Orthogonalized linear combination of atomic orbitals (OLCAO) [2]:**
  - Efficient for complex and large systems
  - Total Bond Order Density, $TBOD = \frac{TBO}{Volume}$
  - Using stress-strain relationship C_{ij} values are obtained and then mechanical properites calculated using VRH approximation.

[1] Kresse, G., Software vasp, vienna, 1999; g. kresse, j. furthmüller. *Phys. Rev. B*, **1996**, *54*(11), p. 169,
[2] Ching, W.-Y. and P. Rulis, *Electronic Structure Methods for Complex Materials: The orthogonalized linear combination of atomic orbitals*: Oxford University Press, 2012, 0199575800

Modeling Approaches

2. Atomistic Modelling Approach

- EAM potential for Ni-Al constructed by Mishin and Purja Pun*
- Interatomic Potential Development of $M_{23}C_6$ using MEAMFIT

Molecular Dynamics Simulation:

- Uniaxial compression test using MD code of LAMMPS
- Relaxed before loading until equilibrium reached.
- Strain rate used $5X10^{9}s^{-1}$, Temperature used 300K
- Used Open Visualization Tool (OVITO) to observe structural evaluation.
- Used Common Neighbor Analysis (CAN) and Dislocation Extraction Algorithm (DXA) tool to analyze dislocation dynamics.

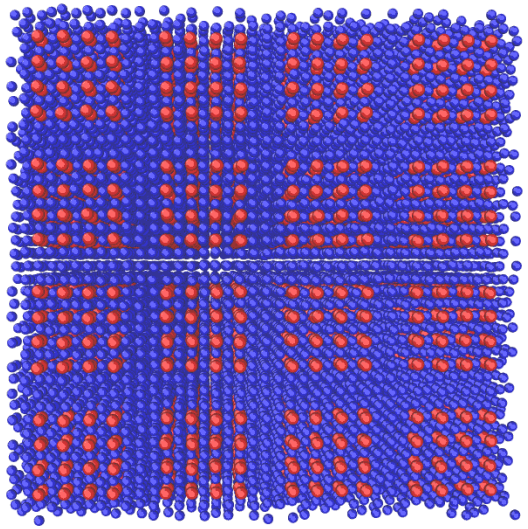

NPT at 1000K

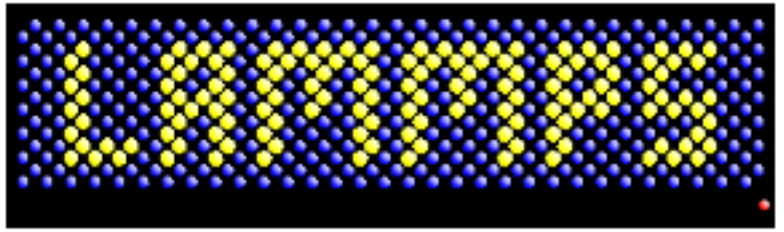

OVITO
Open Visualization Tool

Modeling Approaches

3. Crystal Plasticity & Void Modelling Approach

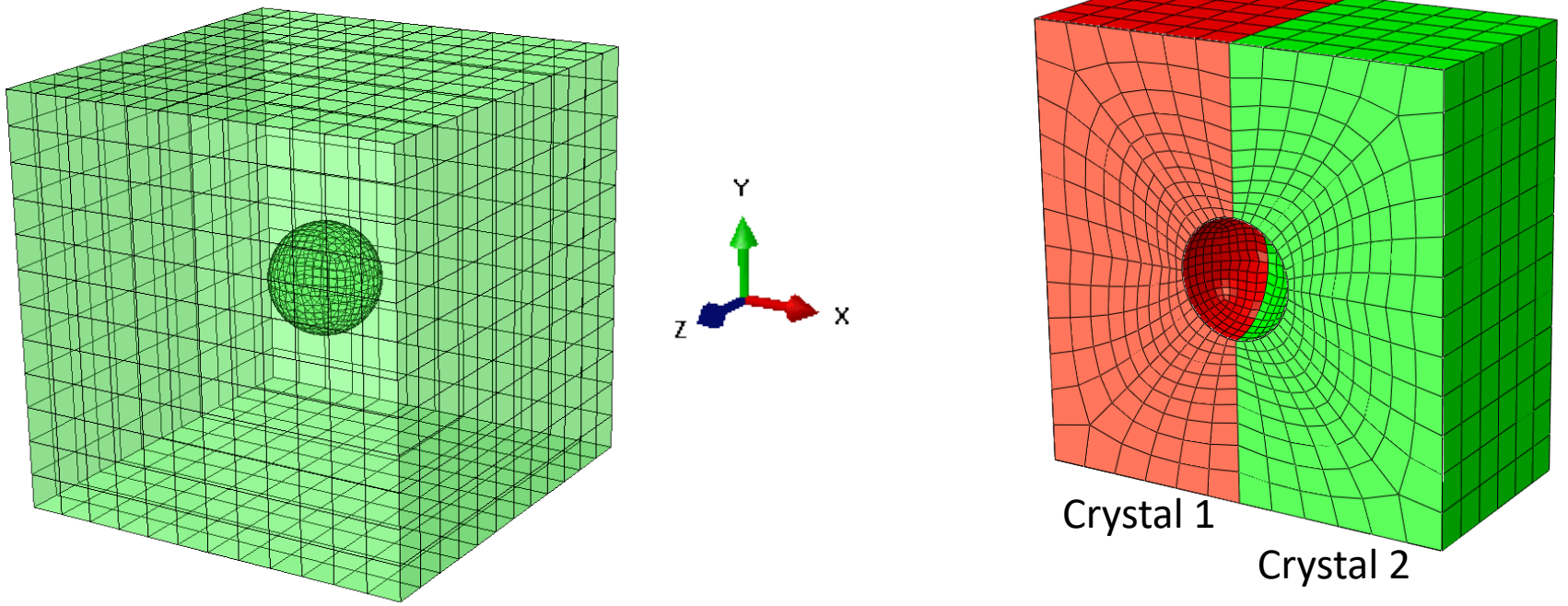

(left) The whole cubic unit cell meshed with 6128 C3D8R elements. (right) Cross-section of the meshed sample (Grain boundary types: Twist 15° & 45° , Tilt 15° & 45°).

The initial void volume fraction, f_0 = 0.01. We focus on the deformation and void growth in Crystal 1.

Electronic structure and elastic properties of crystalline precipitate phases $M_{23}C_6$ (M = Cr, W, Mo, Fe)

- Superalloys contains crystalline precipitates at the grain boundaries or defective sites.
- These precipitates phase have a certain impact on their properties.
- One of precipitate phases of Ni-based superalloys are fcc carbides $M_{23}C_6$ (M= transition metal such as Cr, Mo, W and Fe)

- We investigate this phase with four different transition metals M = Cr, Mo, W and Fe leading to four binary carbides
- Their half-half mixtures of (Cr, Mo), (Mo, W), (Cr, W), (Cr, Fe), (Mo, W), (Mo, Fe), (W, Fe) leading to six ternary carbides.
- Also, four binary nitrides ($M_{23}N_6$).

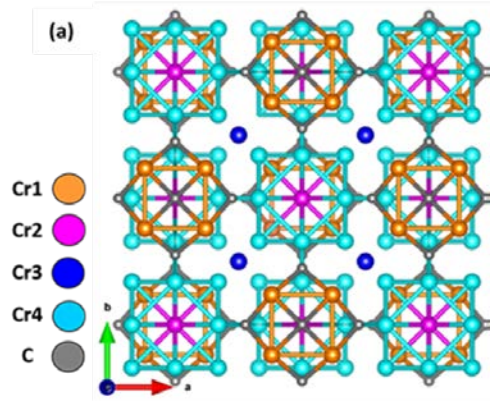

$Cr_{92}C_{24}$
Space Group = 225 (fcc)
Number of atoms =116

Electronic Structure Calculation Approach

Electronic structure and elastic properties of crystalline precipitate phases $M_{23}C_6$ (M = Cr, W, Mo, Fe)

Name: $Cr_{23}C_6$
Lattice parameter:
a = 10.52Å
γ = 90.00°
Space Group: 225
Number of Atom: 116
Types: 5
cell volume = 1165.36 Å^3

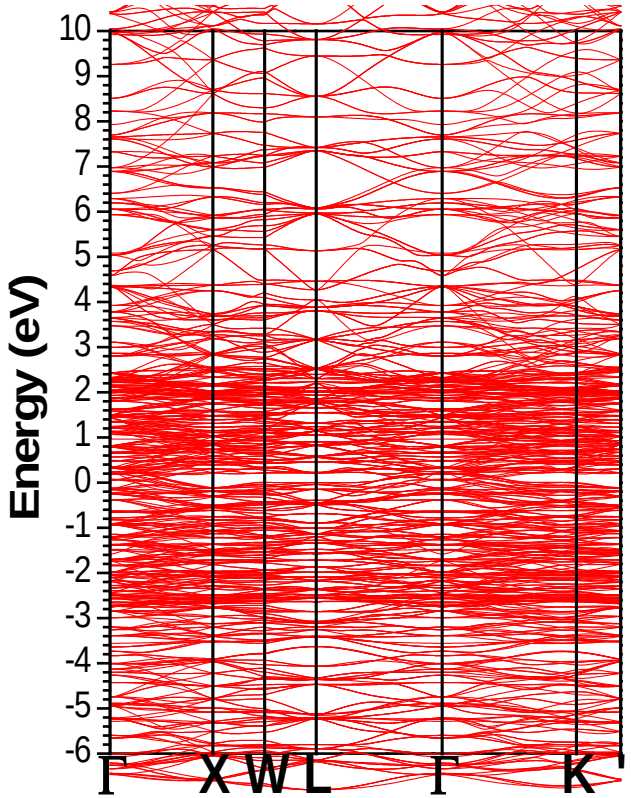

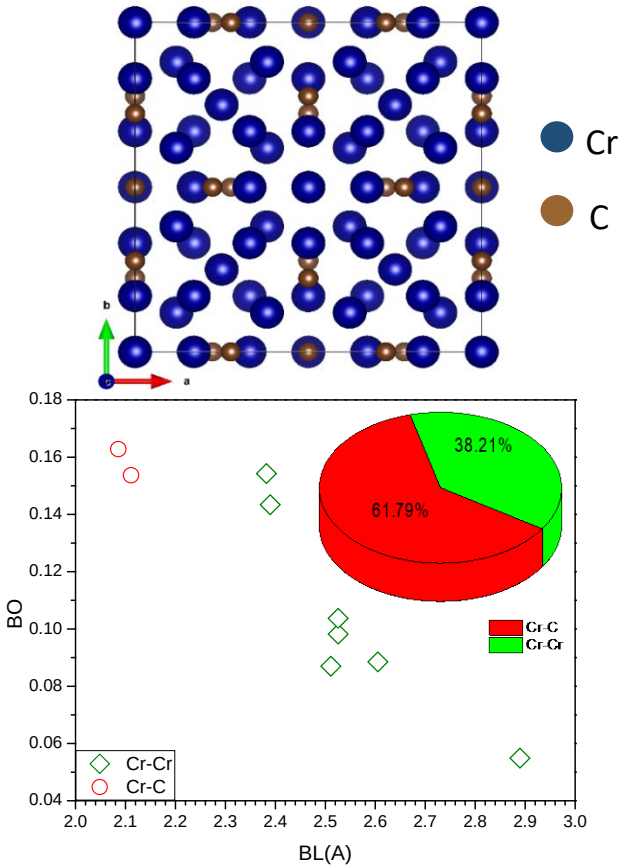

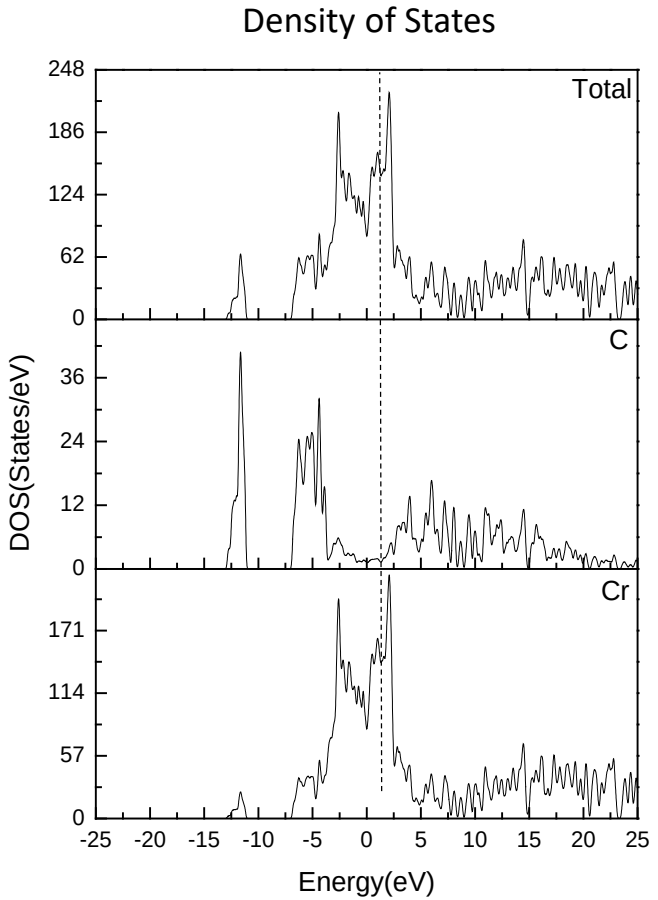

Fundamental elastic Properties

C_{11}	C_{12}	C_{44}	K(GPa)	G(GPa)	E(GPa)	H(GPa)	G/K
472.36	211.46	124.30	298.43	126.63	332.82	0.31	0.42

Electronic Structure Calculation Approach

Electronic structure and elastic properties of crystalline precipitate phases $M_{23}C_6$ (M = Cr, W, Mo, Fe)

$N(E_F) = 84.4$ 242.7 67.8 61.1

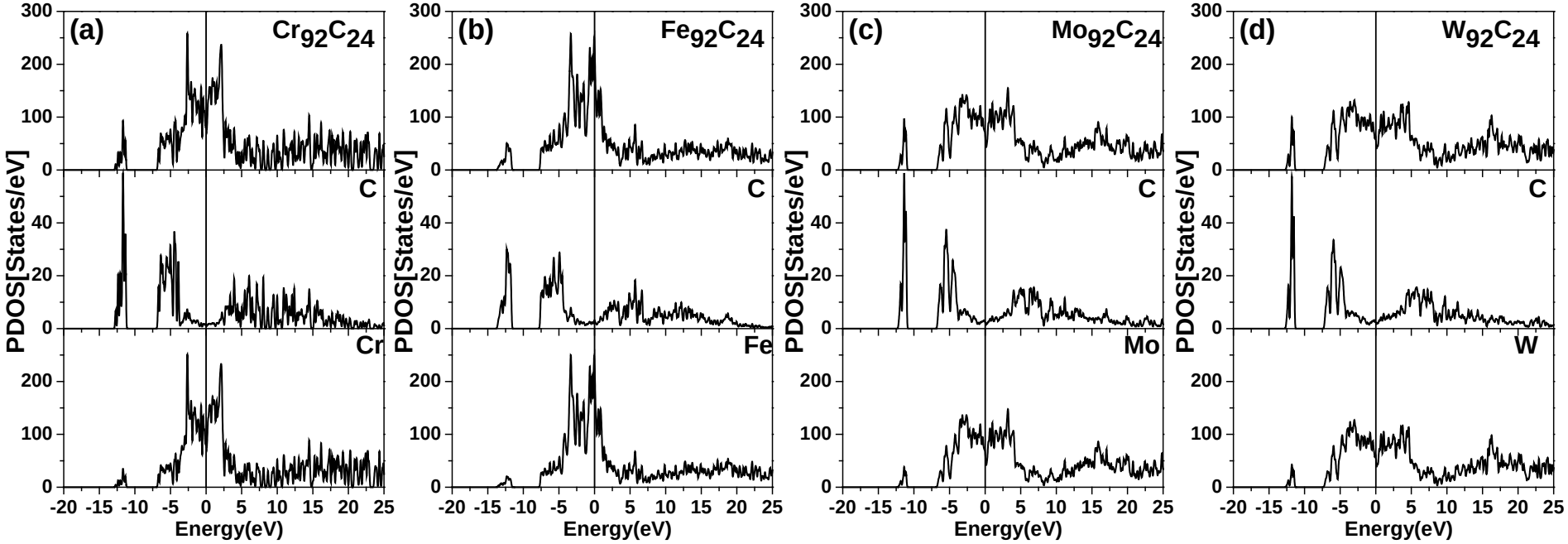

Total density of states and partial density of states of binary carbides.

In binary carbides,

- $W_{92}C_{24}$ to be the most stable.
- $Fe_{92}C_{24}$ to be the least stable.

In ternary carbides (not shown here)

- $Mo_{46}W_{46}C_{24}$ most stable
- All Fe-containing crystals exhibit higher $N(E_F)$

Electronic Structure Calculation Approach

Electronic structure and elastic properties of crystalline precipitate phases $M_{23}C_6$ (M = Cr, W, Mo, Fe)

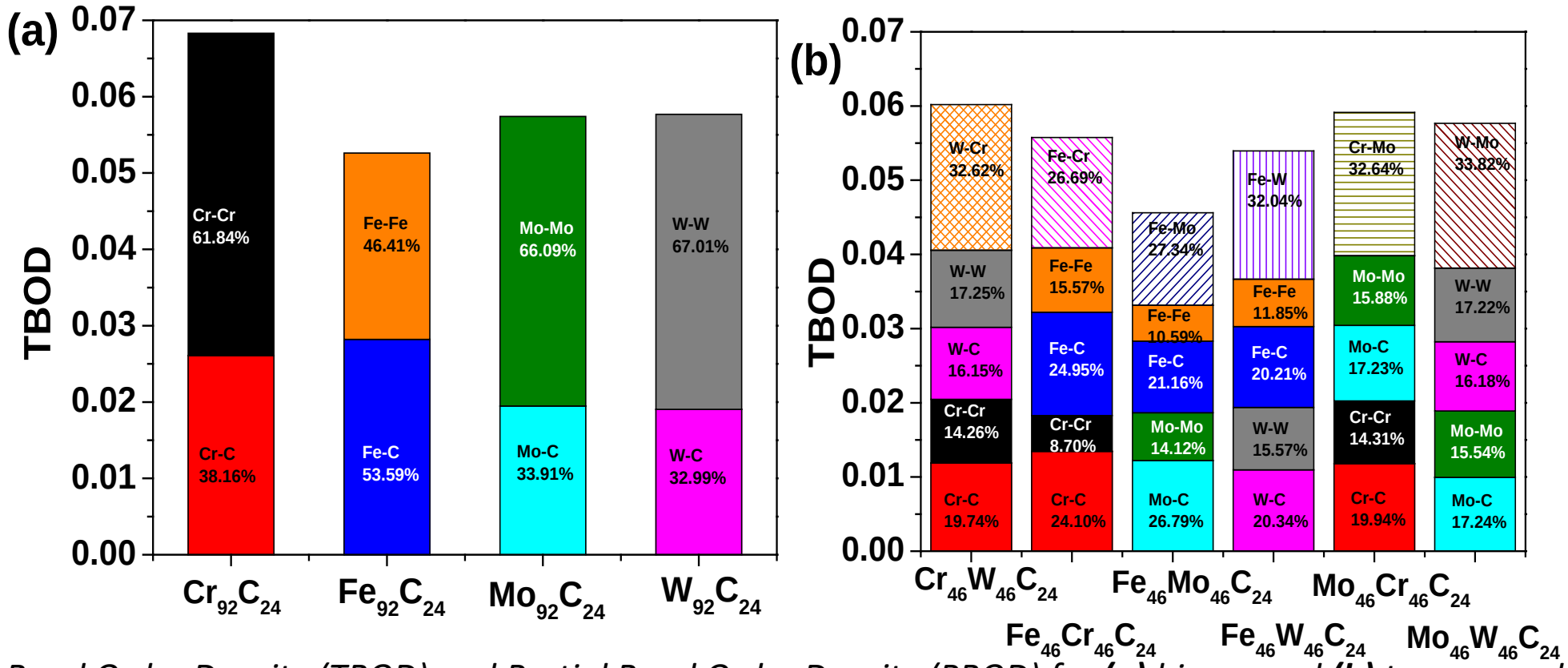

*Total Bond Order Density (TBOD) and Partial Bond Order Density (PBOD) for **(a)** binary and **(b)** ternary carbides*

- Dominance of d-metal + d-metal interactions
- $Cr_{23}C_6$ is the most cohesive phase compared to other binary and ternary carbides.
- Fe-containing carbides tends to make them much less cohesive.

Electronic Structure Calculation Approach

Electronic structure and elastic properties of crystalline precipitate phases $M_{23}C_6$ (M = Cr, W, Mo, Fe)

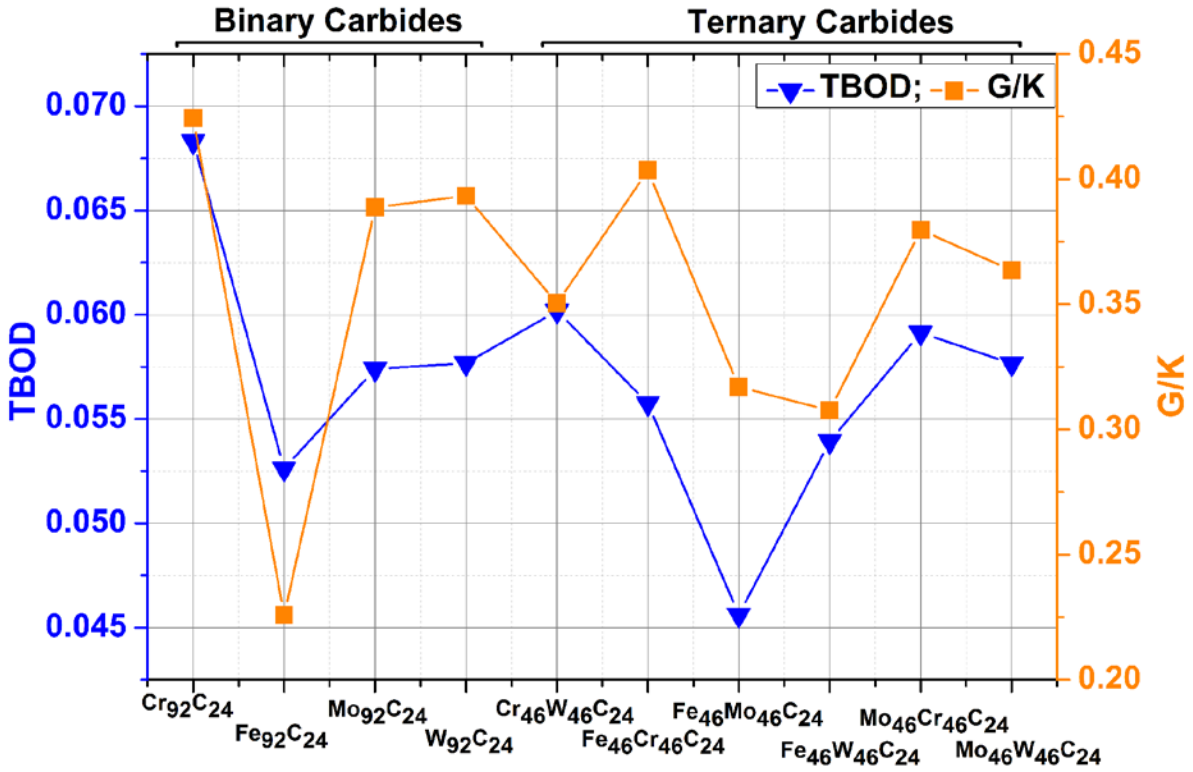

- Except $Cr_{46}W_{46}C_{24}$, the TBOD and G/K ratio follows similar pattern showing the good correlation among them.
- Our analysis validates the relation between the electronic structure, TBOD and mechanical properties in $M_{23}C_6$ for the first time.

Electronic structure and elastic properties of crystalline precipitate phases $M_{23}C_6$ (M = Cr, W, Mo, Fe)

Conclusion: Electronic Structure Calculations

- Deep valley in the DOS at Fermi level and the lower values for $N(E_F)$ in these crystals except for M = Fe.
- Both Fe-containing binary carbides and nitrides are less stable due to weaker Fe-Fe bonding.
- The replacement of C by N results in slight decrease in crystal cohesion and mechanical properties.
- The effective use of TBOD as a single parameter to characterize the crystal cohesion.
- The $Cr_{23}C_6$ as the most effective precipitate phase in Ni-super alloys.
- Evidence of positive correlation between electronic structure, TBOD and mechanical properties (especially G/K) in these complex crystals

Atomistic Modelling Approach

EAM Interatomic Potential Development for MC Systems

$$E_{tot} = \frac{1}{2}\sum_{i,j}\phi_{ij}(r_{ij}) + \sum_{i}F_i(\overline{\rho_i})$$

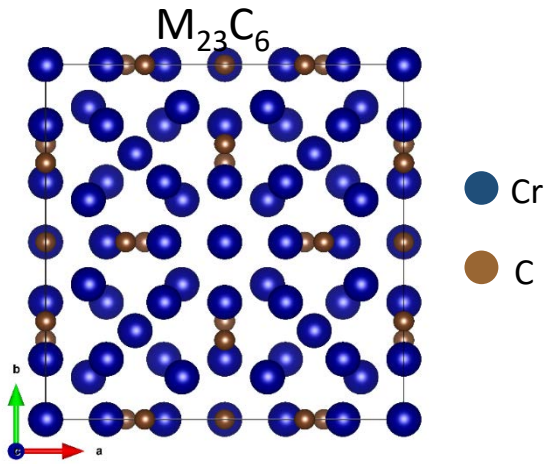

$\phi_{ij}(r_{ij})$ → **Pair Potential**

$F_i(\overline{\rho_i})$ → **Embedding energy**

$\overline{\rho}_i = \sum_{j\neq i}\rho_i(r_{ij})$ → **Atomic density function**

DFT Samplings (force,energy &stress) from $M_{23}C_6$ ONLY

↓

Force Fitting code MEAMFIT

↓

EAM

MEAMFIT: Andrew Ian Duff ,M.W. Finnis, Philippe Maugis, Barend J. Thijsse, Marcel H.F. Sluiter, *Computer Physics Communications* 196 (2015) 439–445

Atomistic Modelling Approach

EAM Interatomic Potential Development for MC Systems

$Cr_{23}C_6$

1500K

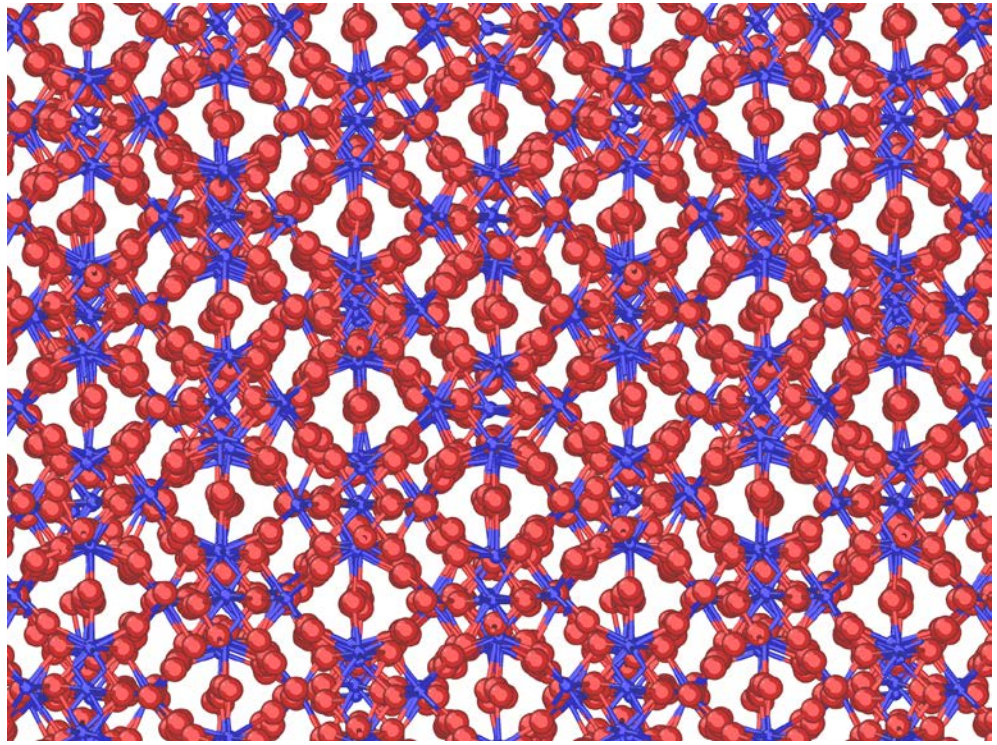

$W_{23}C_6$

2000K

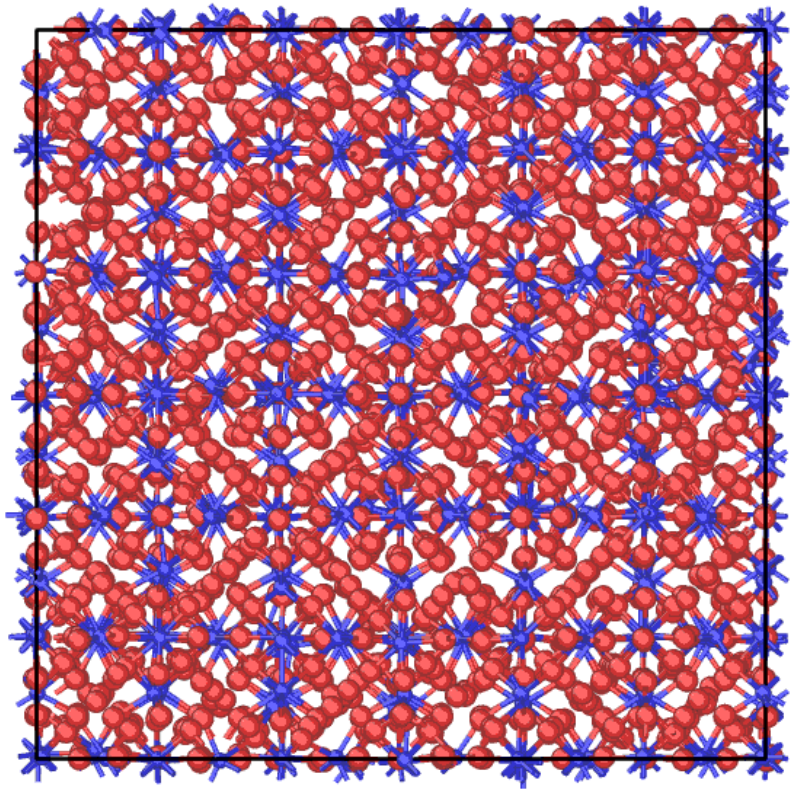

Atomistic Modelling Approach

New Transferable EAM Many-body Potentials in Carbide Systems

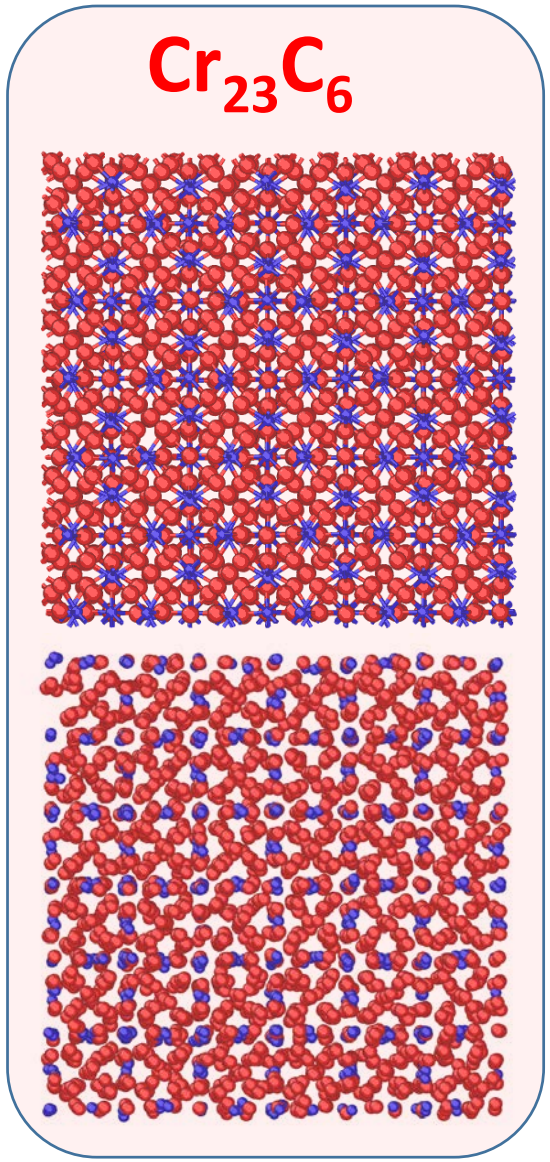

Atomistic Modelling Approach

Role of Void Dynamics

Evolution of damage:

$$\frac{dD}{dt} = \beta \dot{\varepsilon}_o \left[\frac{1}{(1-D)^n} - (1-D)\right]\left(\frac{\sigma_e}{\sigma_0}\right)^n$$

σ_e = equivalent stress n = power law exponent

A. C. F. Cocks and M. F. Ashby. On creep fracture by void growth. *Progress in Materials Science*, 27:189–244, 1982.

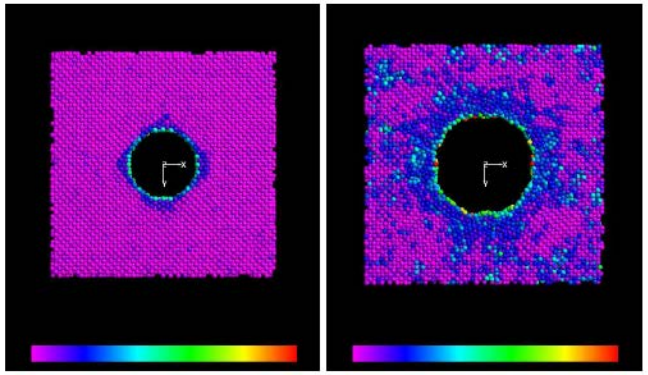

) Prismatic dislocation (0.9 ps) (b) Growing defects (1.7 ps)

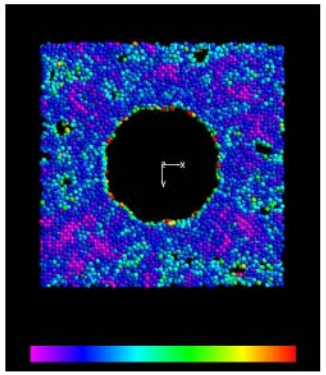

(c) Void nucleation (2.0 ps)

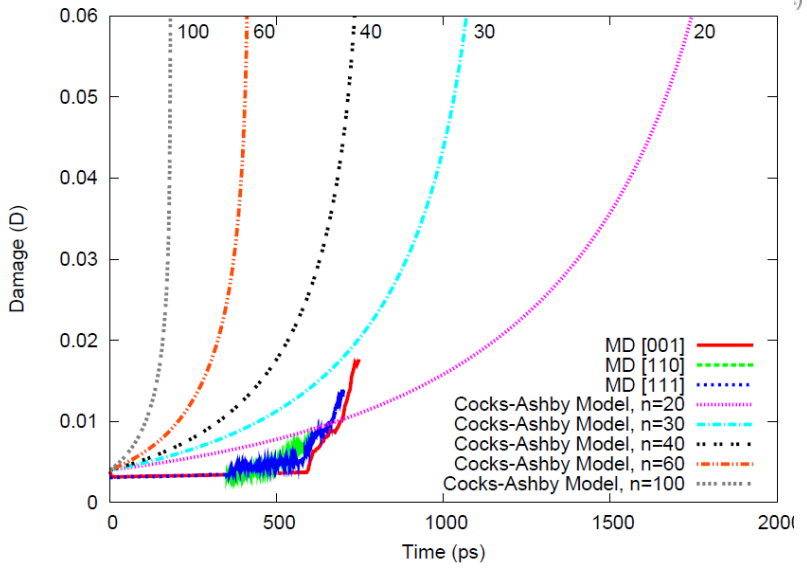

Traiviratana, Sirirat, A molecular dynamics study of void initiation and growth in monocrystalline and nanocrystalline copper, PhD Thesis, UC San Diego 2008 https://escholarship.org/uc/item/6905g1rt

Pure Ni

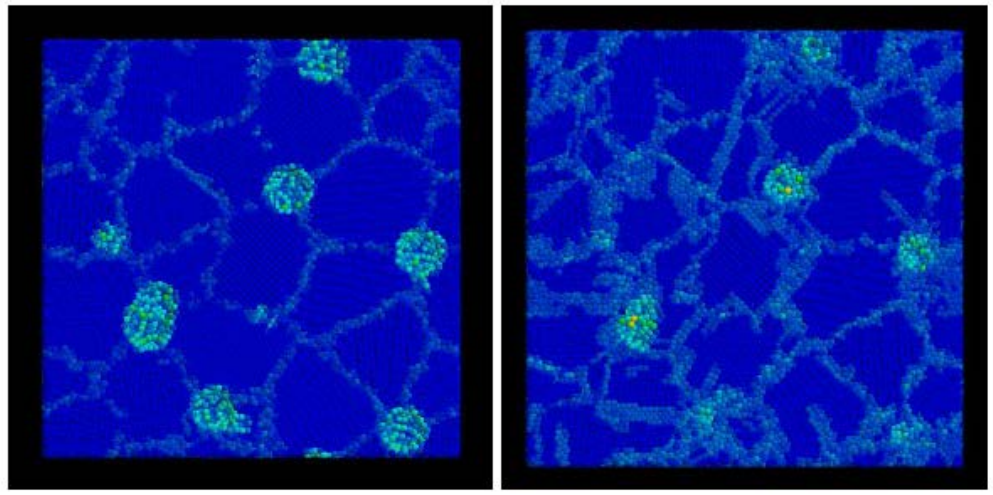

(a) Initial condition (b) Fully loaded

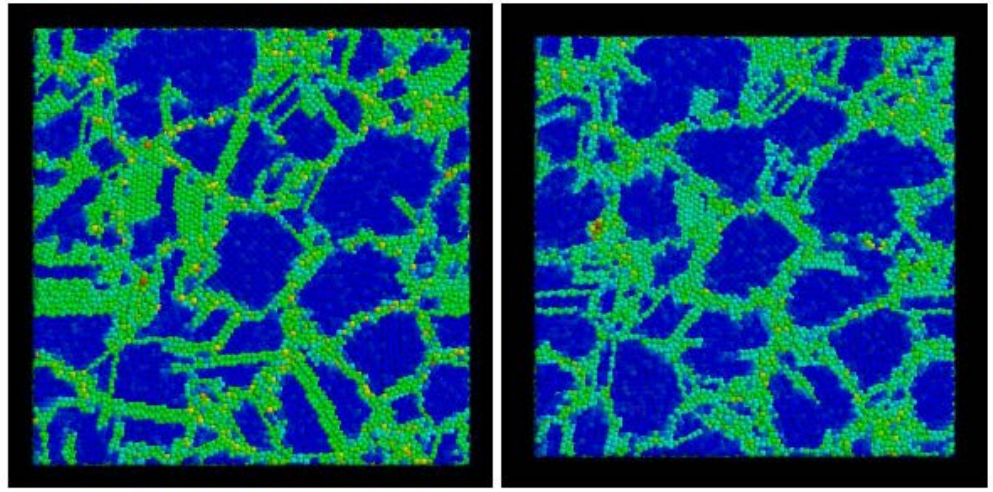

(c) End of holding at constant strain (d) Fully unloaded

Atomistic Modelling Approach

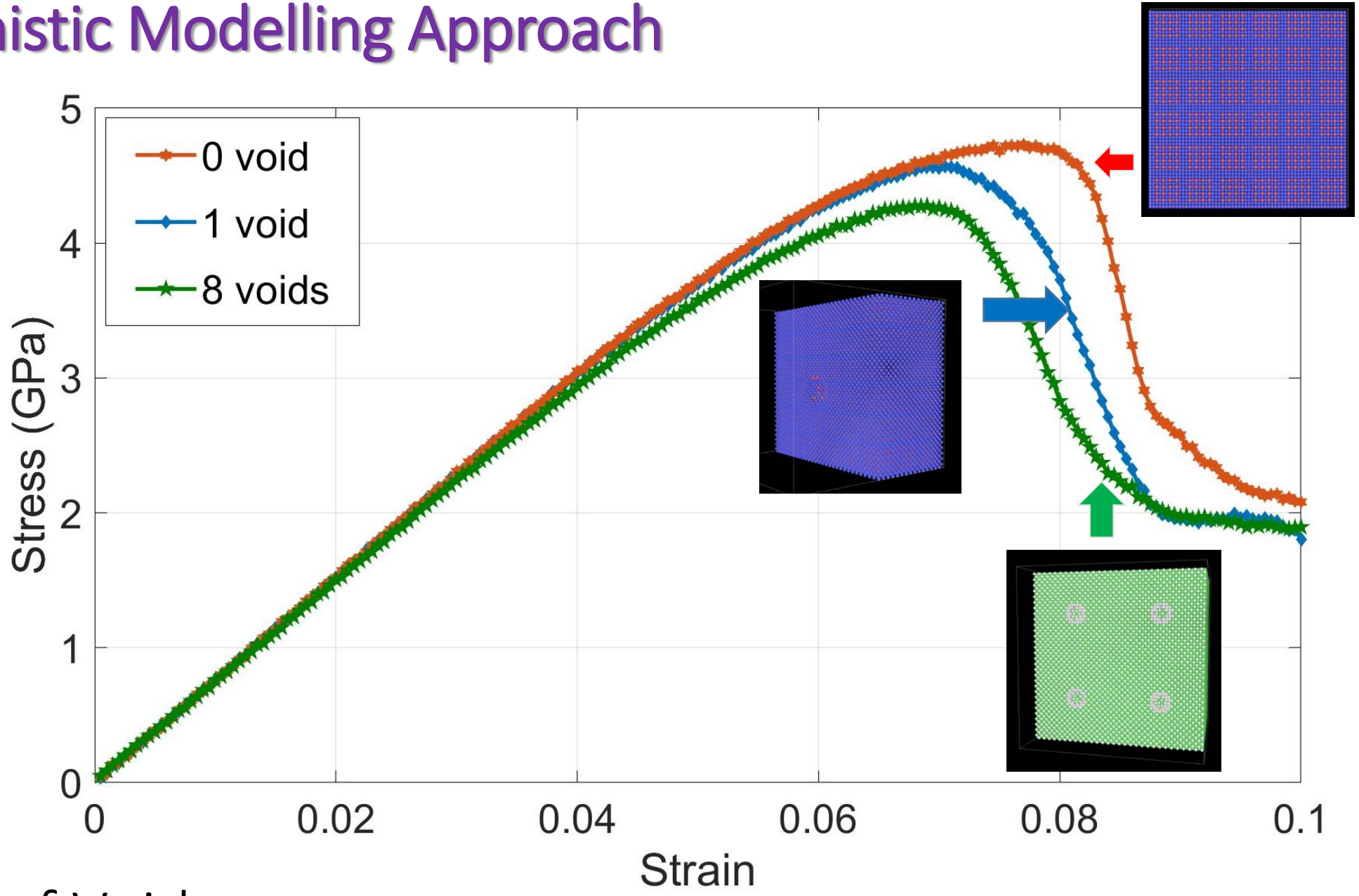

Effect of Voids

Atomistic Modelling Approach

- Presence of void makes the dislocation earlier.
- More # voids ➔ easier dislocation nucleation
- Voids act as dislocation nucleation center.
- Dislocation starts from void surface.

Effect of Voids

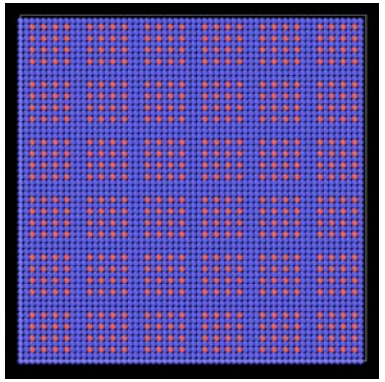

Without void
(6ps to 11ps)

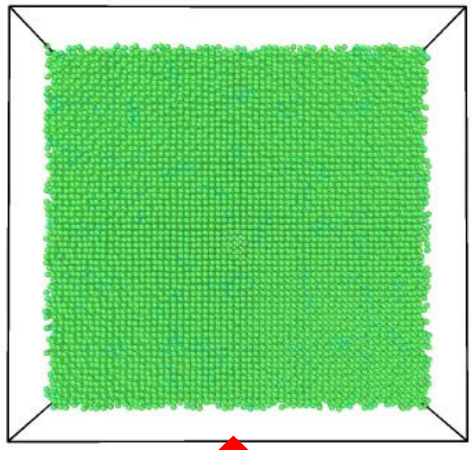

Dislocation Starts

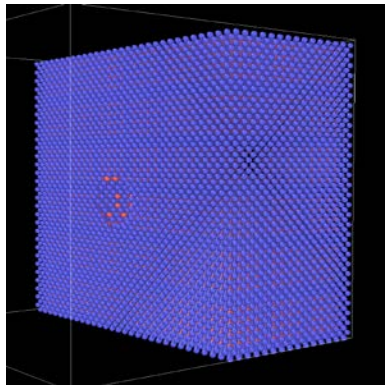

Single void in the middle
(6ps to 11ps)

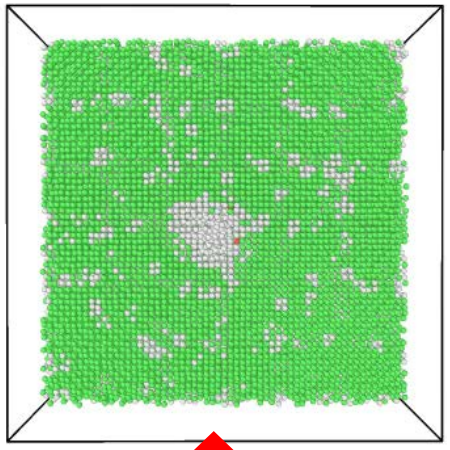

Dislocation Starts

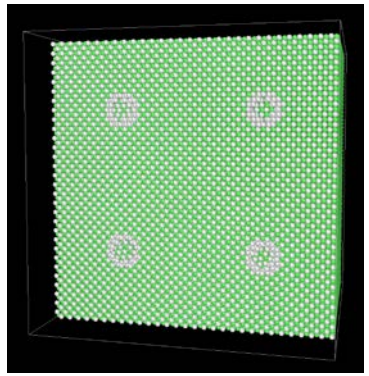

Eight (8) discrete voids
(6ps to 11ps)

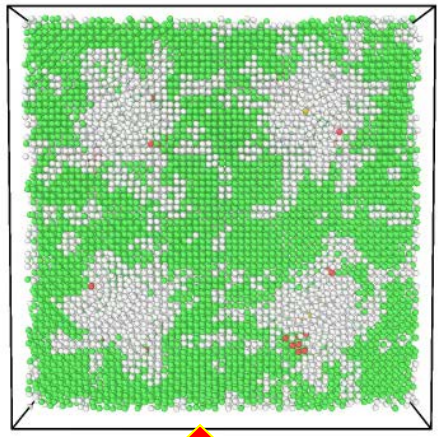

Dislocation Starts

Atomistic Modelling Approach

Effect of Voids

For sample with no void

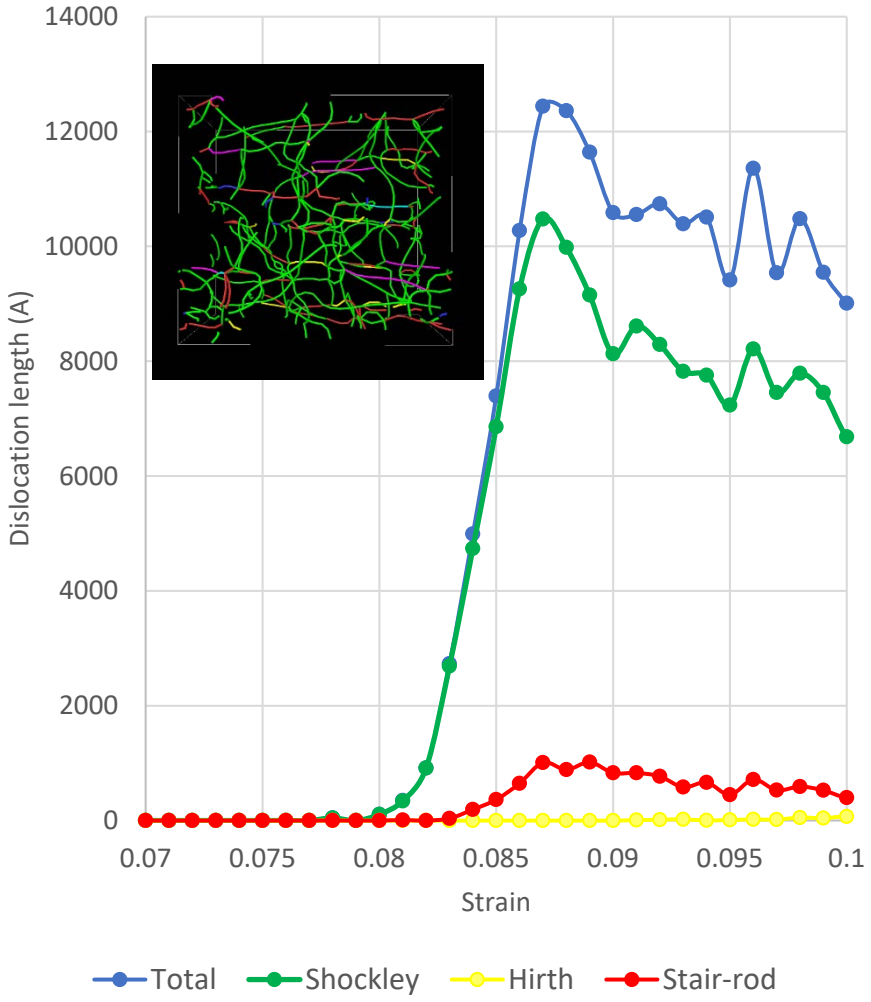

For sample with single void

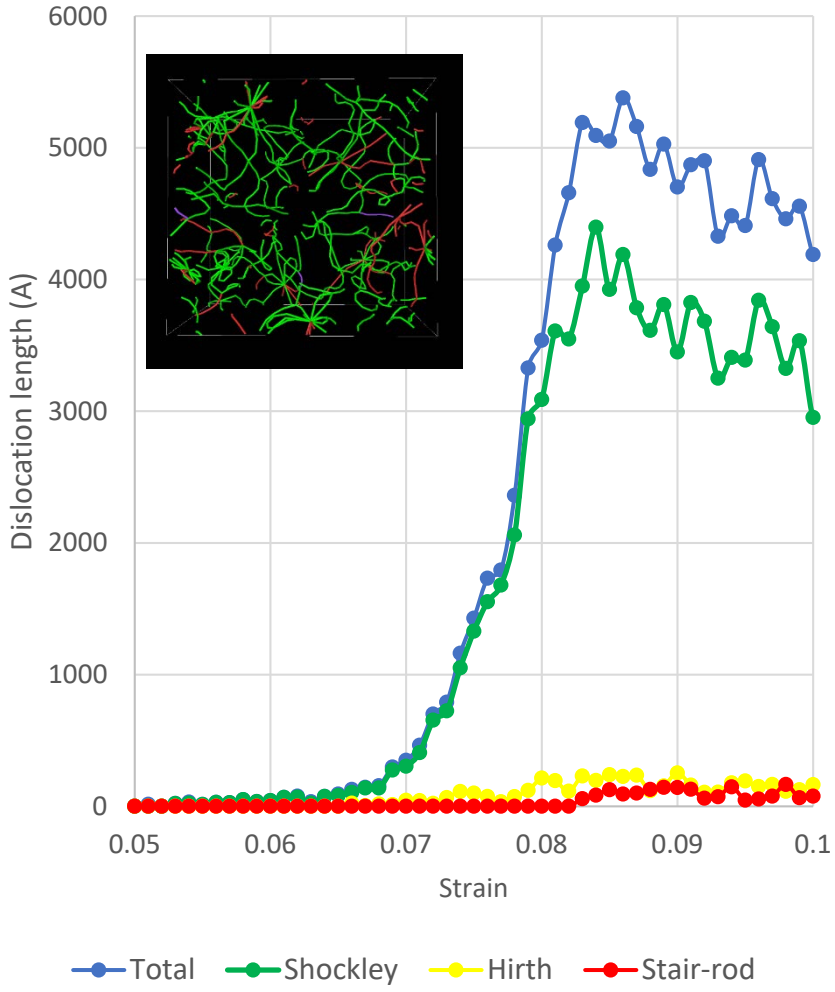

For sample with multiple voids

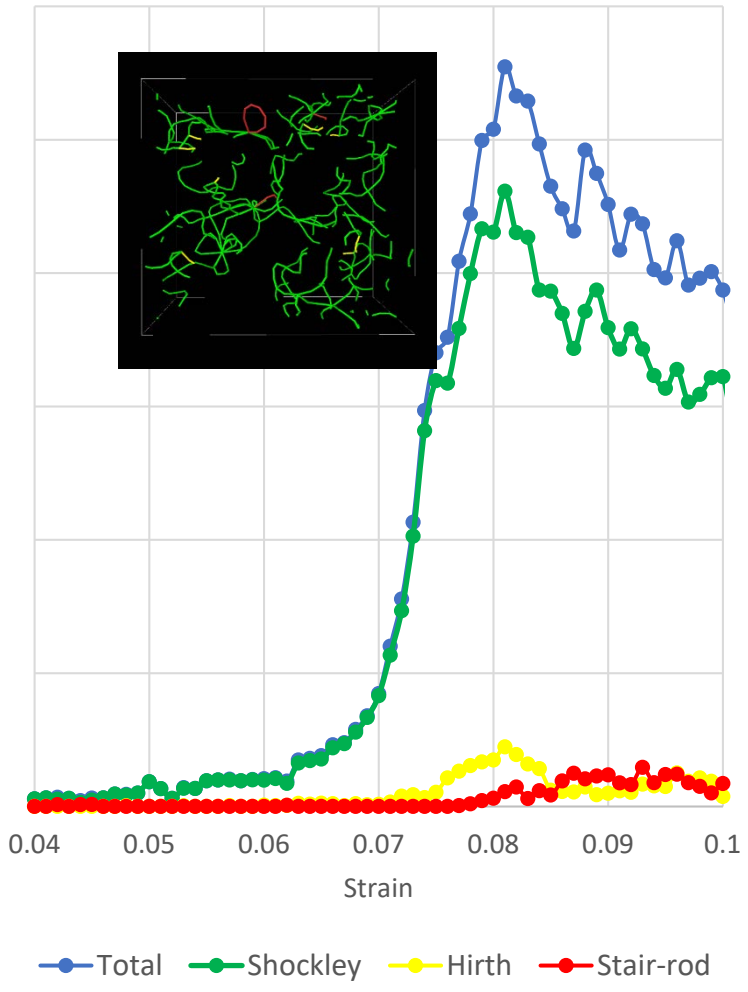

Atomistic Modelling Approach

Distribution of Gamma-Prime Phases

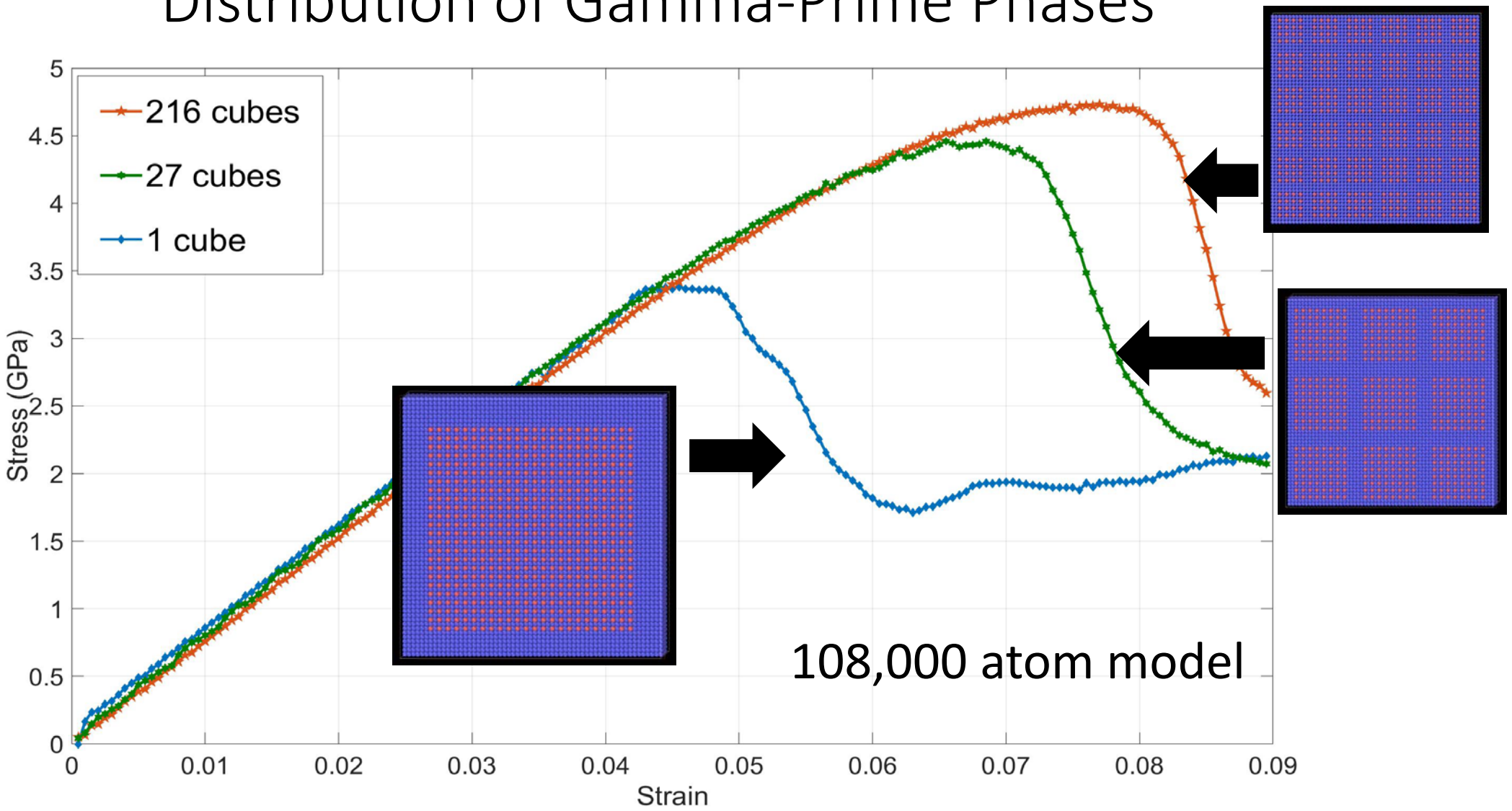

Role of Contiguity

Atomistic Modelling Approach

Conclusion: Molecular Dynamics Simulation

- Developed new and transferable EAM potentials to model carbide systems.

- Assessed roles of voids & γ’ distribution in deformation mechanism in a model γ + γ’ system.

- Analyze the dislocation dynamics within the model system during deformation ➔ polycrystalline models.

Crystal plasticity finite element method

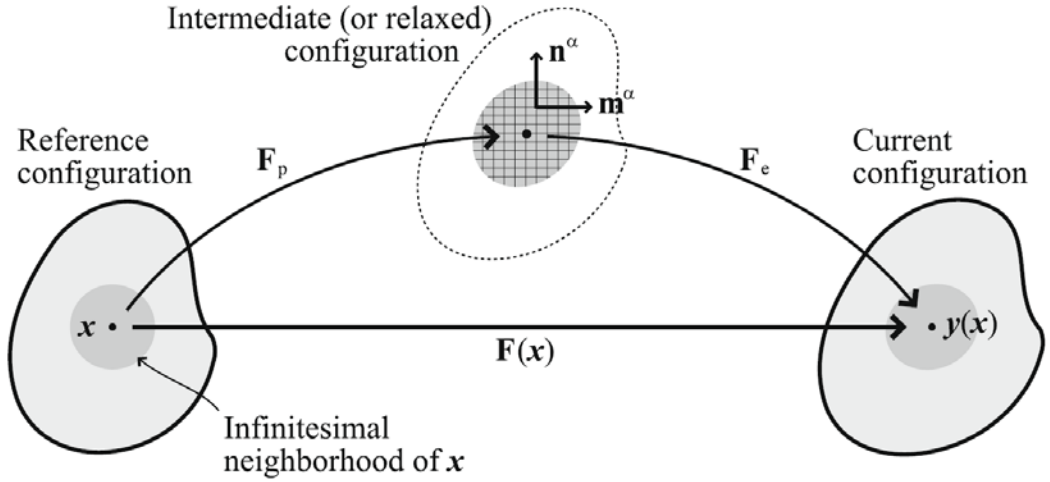

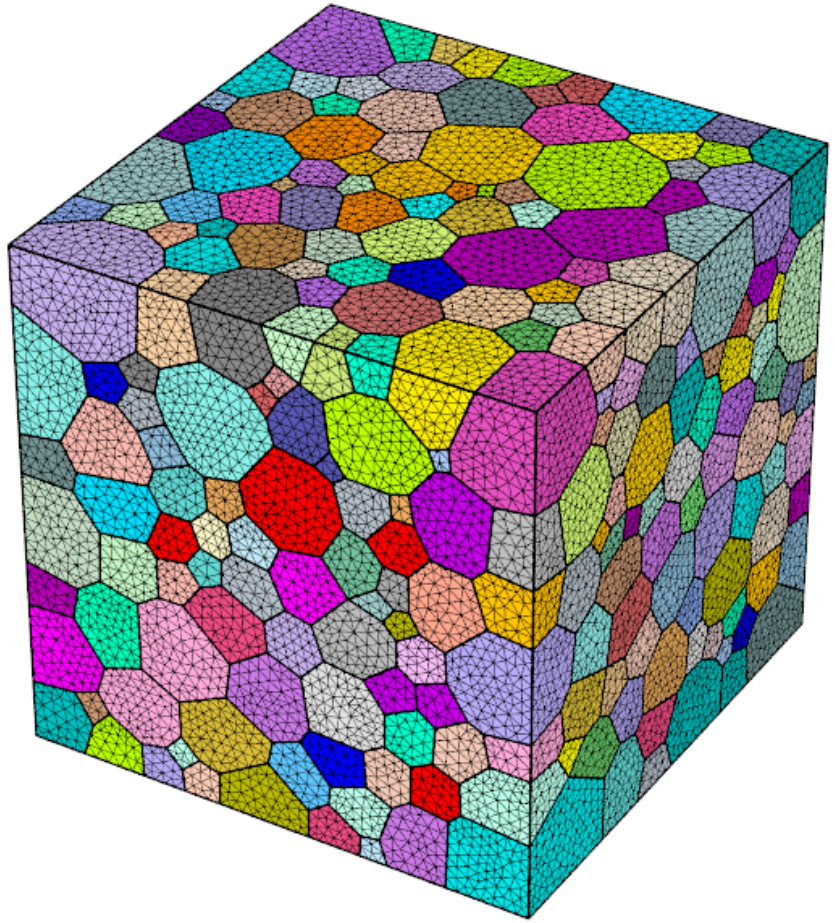

The **plastic part** of the velocity gradient, $\boldsymbol{F}^p$, is

$$\boldsymbol{F}^p = \sum_{\boldsymbol{\alpha}} \dot{\boldsymbol{\gamma}}^{\boldsymbol{\alpha}} \mathbf{b}^{\boldsymbol{\alpha}} \otimes \mathbf{n}^{\boldsymbol{\alpha}}$$

$$\dot{\boldsymbol{\gamma}}^{\boldsymbol{\alpha}} = \dot{\gamma}_0^{\alpha} \left(\frac{|\tau^{\alpha}|}{\tau_c^{\alpha}} \right)^{\frac{1}{m}} sign(\tau^{\alpha})$$

$\dot{\boldsymbol{\gamma}}^{\boldsymbol{\alpha}}$ is the shear strain rate in slip system α

$\boldsymbol{\tau}^{\boldsymbol{\alpha}}$ is the resolved shear stress (RSS) in slip system α

τ_c^{α} is the critical resolved shear stress (CRSS) for a particular slip event

$\dot{\gamma}_0$ is a reference shear strain rate

m is the strain rate sensitivity

Crystal plasticity finite element method

Strain hardening and plastic flow rule

Voce-type strain hardening crystal plasticity model:

$$\dot{\tau}_c^{\alpha} = \sum_{\beta} h_{\alpha\beta} \left|\dot{\gamma}^{(\beta)}\right|$$

$$h_{\alpha\beta} = q_{\alpha\beta} * h$$

$\dot{\gamma}^{\beta}$ is the shear strain rate in slip system β

$h_{\alpha\beta}$ - strain hardening modulus of self and latent hardening

$q_{\alpha\beta}$ are the interaction coefficients

$$h = h_s + \left[h_0 - h_s + \frac{h_0 h_s \gamma_\alpha}{\tau_s - \tau_0}\right] exp^{-\frac{h_0 \gamma_\alpha}{\tau_s - \tau_0}}$$

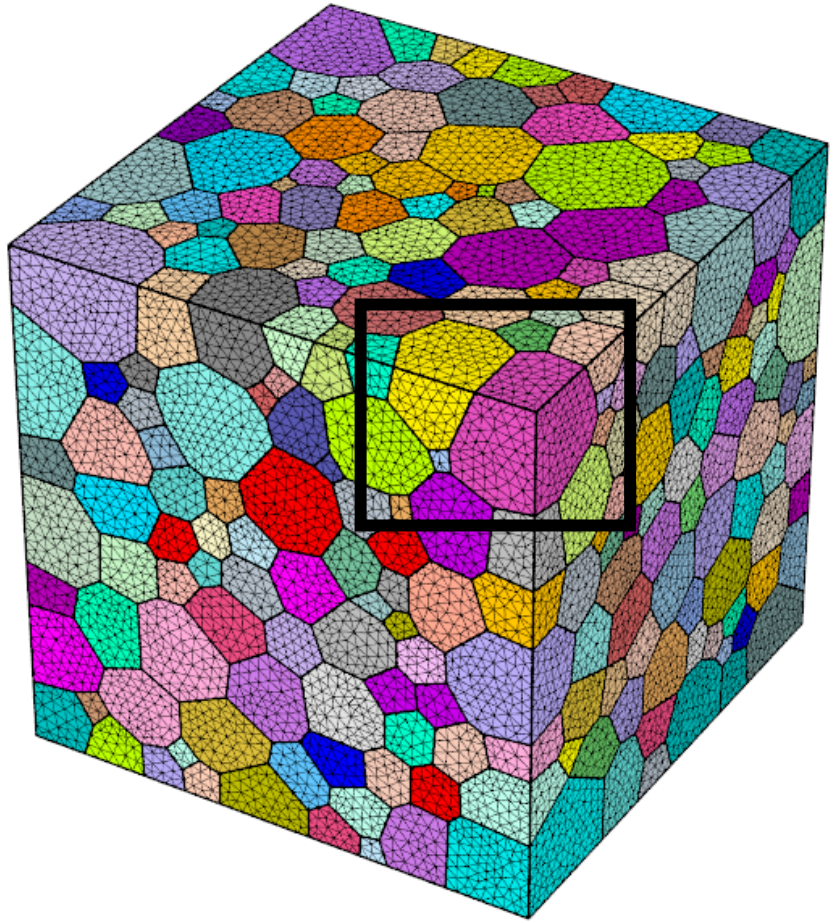

h_s is the saturation hardening modulus at large strain, $q_{\alpha\beta}$ are the interaction coefficients, h_0 is the initial hardening modulus, τ_0 is the initial yield shear stress, τ_s is the saturation yield shear stress.

Acta Metall. 32 (1984) 1637–1653

Crystal plasticity finite element method

Model parameters from micropillar compression tests

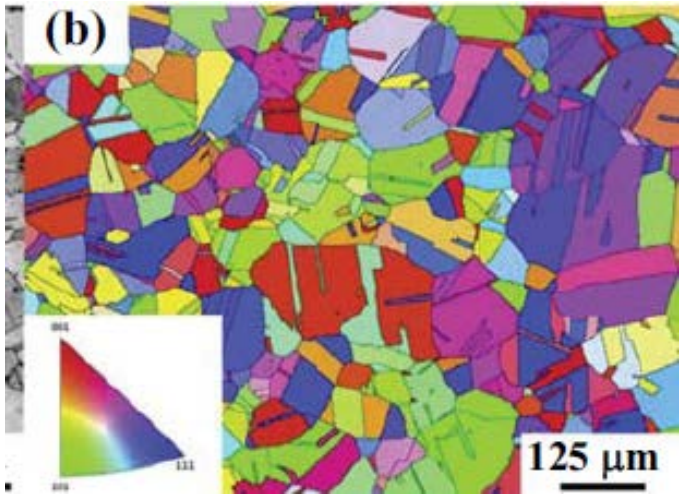

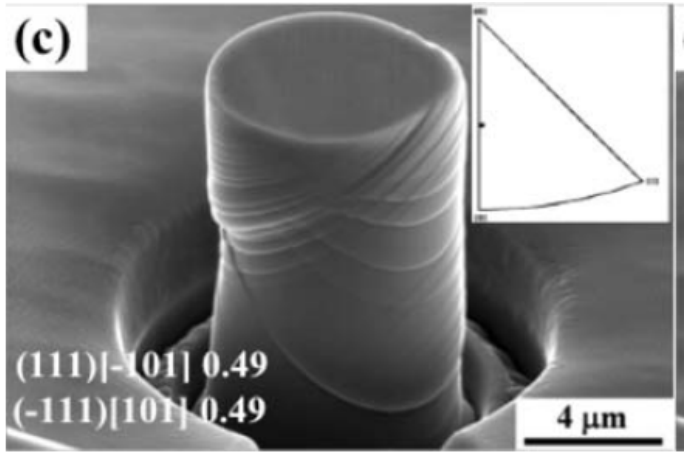

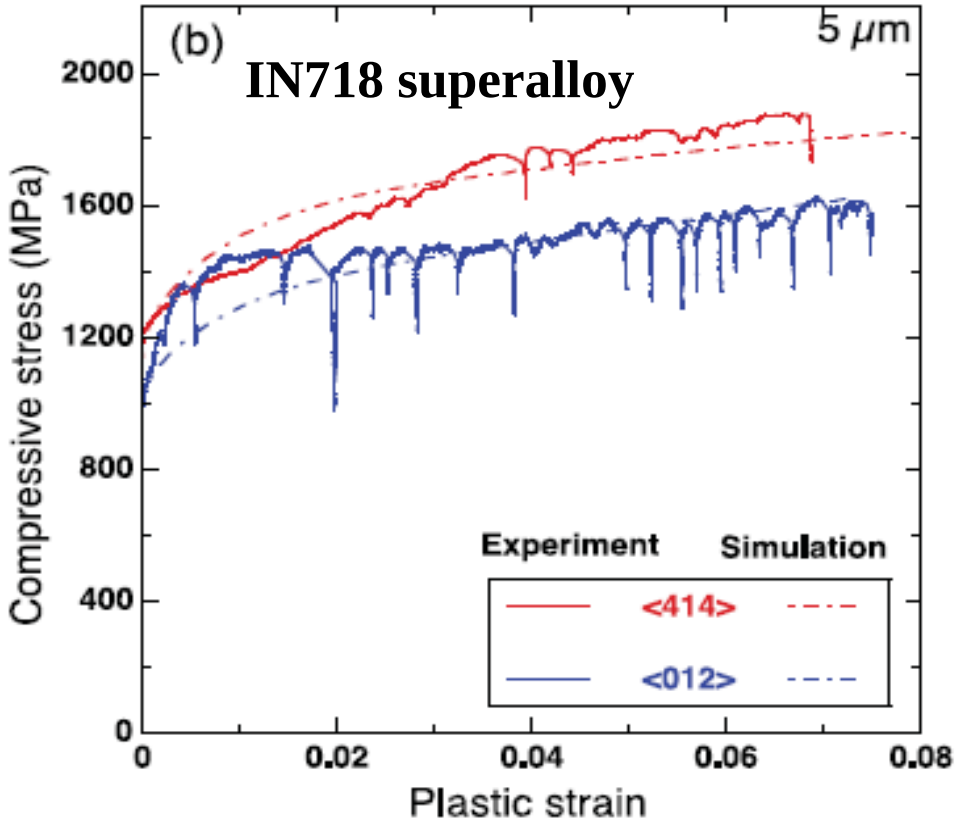

Acta Materialia 98 (2015): 242-253

CPFEM parameters

C_{11}	C_{12}	C_{44}	τ_0	τ_s	h_0	h_s	$q_{\alpha\beta}$
259.6GPa	179 GPa	109.6GPa	465.5 MPa	598.5 MPa	6.0 GPa	0.3 GPa	1

Crystal plasticity finite element method

Classic void growth model

Rice- Tracey model predicts the relationship between the void volume fraction and the stress triaxiality:

$$\frac{dlnf}{d\varepsilon_p} = 0.85e^{1.5T} \qquad T = \frac{\sum h}{\sum e}$$

The ratio of the hydrostatic part of the stress to the equivalent stress.

where f and ε_p are the void volume fraction and equivalent plastic strain, respectively.

The average (hydrostatic) stress and macro-equivalent stress are:

$$\sum h = \frac{1}{3}(\sum 1 + \sum 2 + \sum 3)$$

$$\sum e = \frac{1}{\sqrt{2}}\sqrt{(\sum 1 - \sum 2)^2 + (\sum 2 - \sum 3)^2 + (\sum 3 - \sum 1)^2}$$

Rice, J. R., & Tracey, D. M, Journal of the Mechanics and Physics of Solids, 17(3), 201-217 (1969).

Crystal plasticity finite element method

We applied BCs to get the constant stress triaxilaty during loading

Loading method:

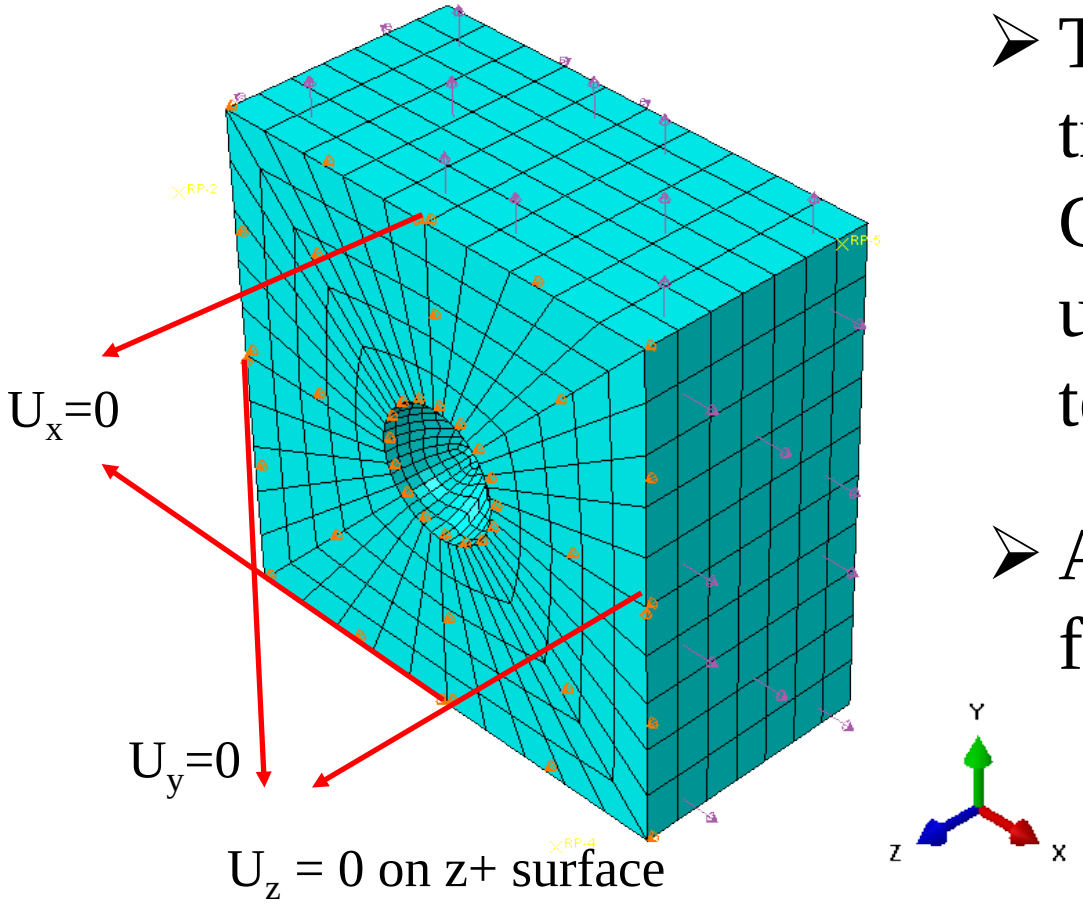

- To systematically analyze how the stress triaxilaity, ***T***, affect the void growth on GBs, four different stress triaxilaity are used in our calculations: 0.33 (uniaxial tension), 0.5, 1.0 and 2.0.
- All six surfaces are constrained to remain flat using MPC (multi-point constraints).

Crystal plasticity finite element method

Void growth in single crystal sample

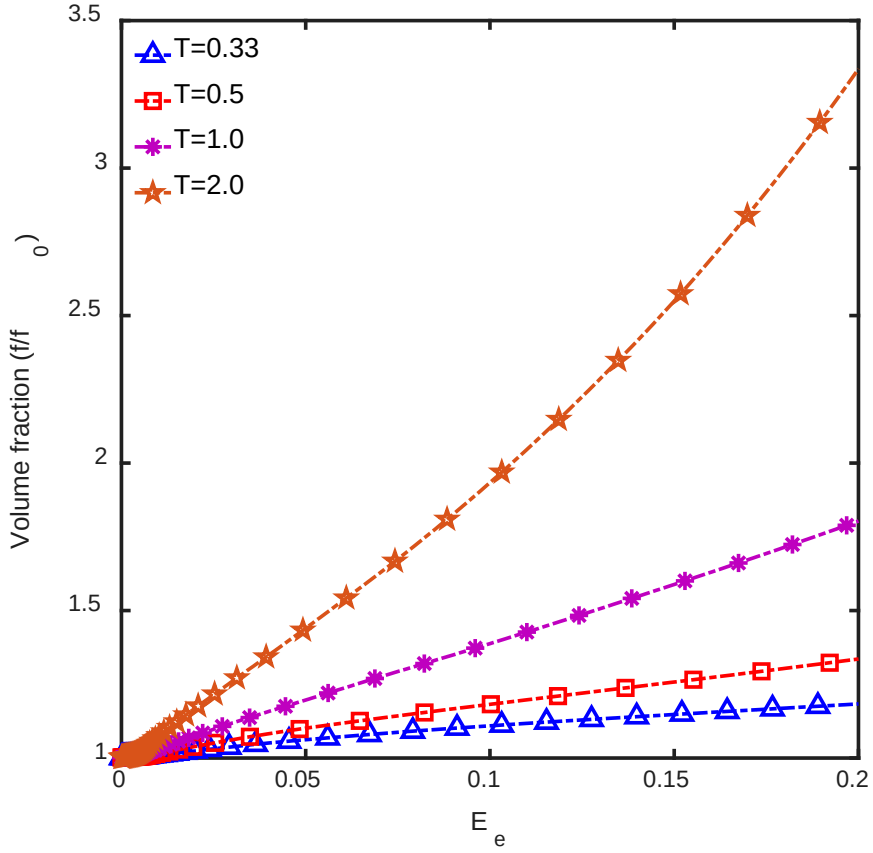

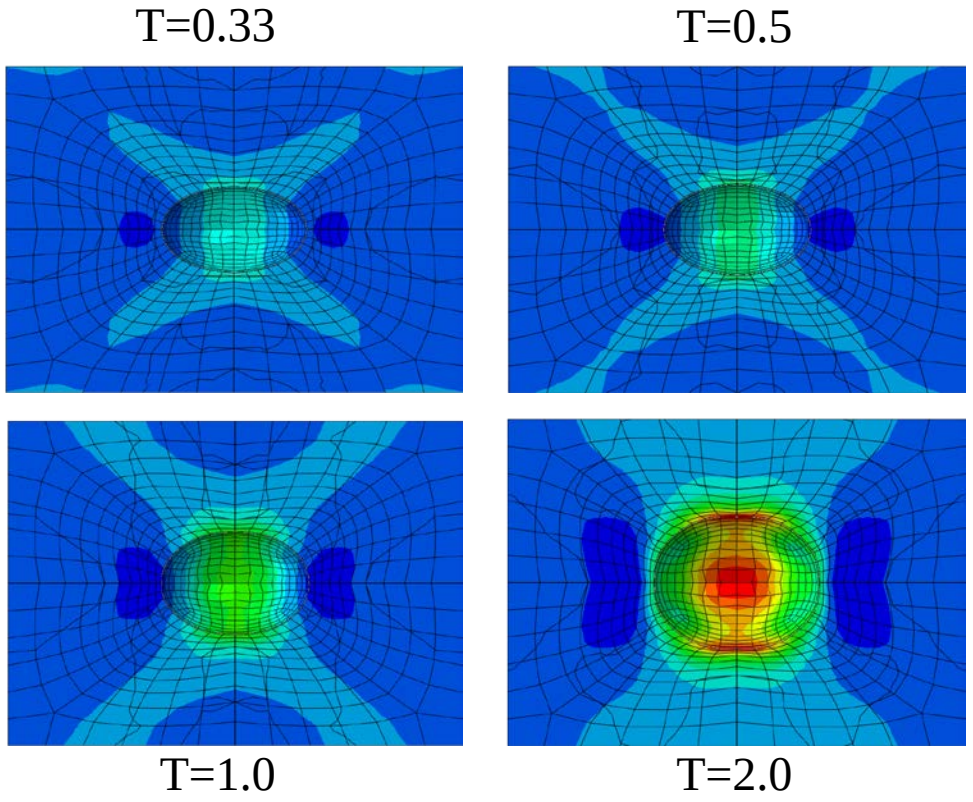

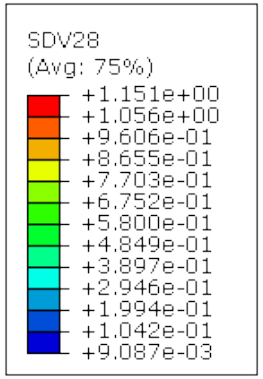

- The void volume increases with the macro-equivalent.
- Higher stress triaxiality induced faster void growth.
- The shape of the void is strongly affected by the stress triaxiality.

Crystal plasticity finite element method

Void shape in bicrystals

T = 0.33

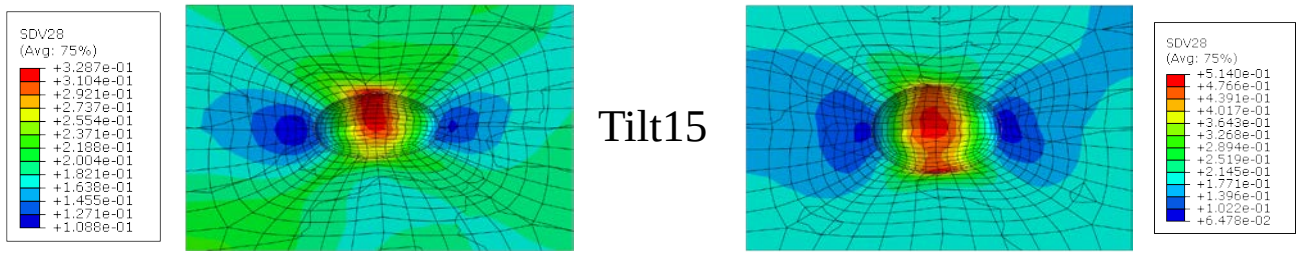

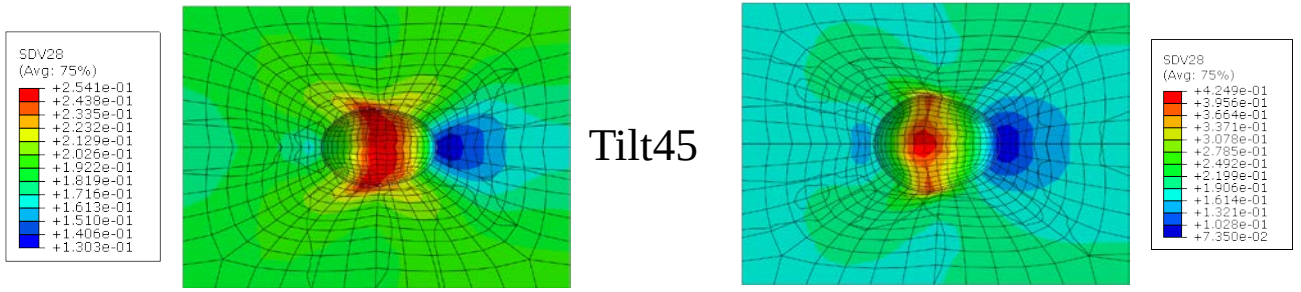

T = 2.0

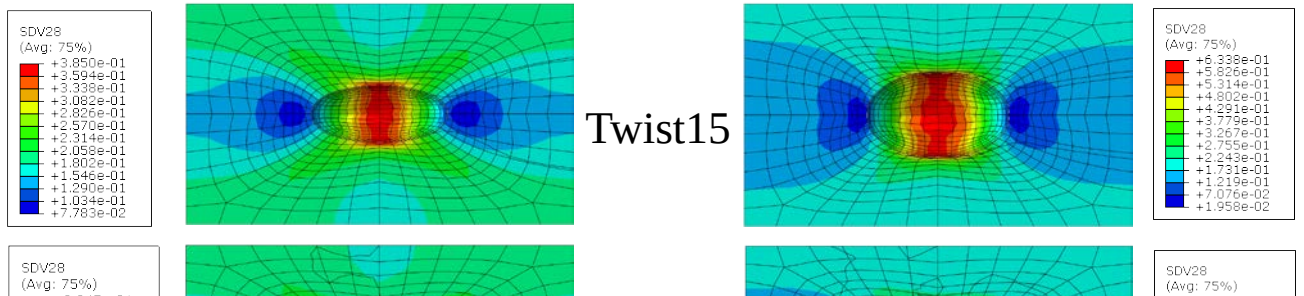

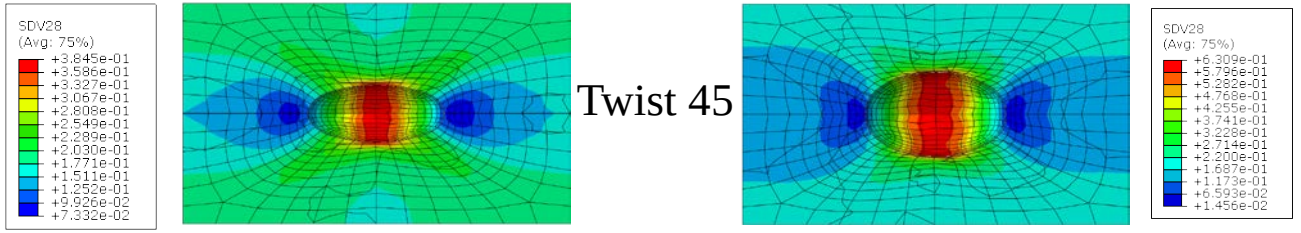

The void volume grew highly unsymmetrically in bicrystals with tilt GBs, while the deformation along twist GBs is symmetrical.

Crystal plasticity finite element method

Single crystal sample

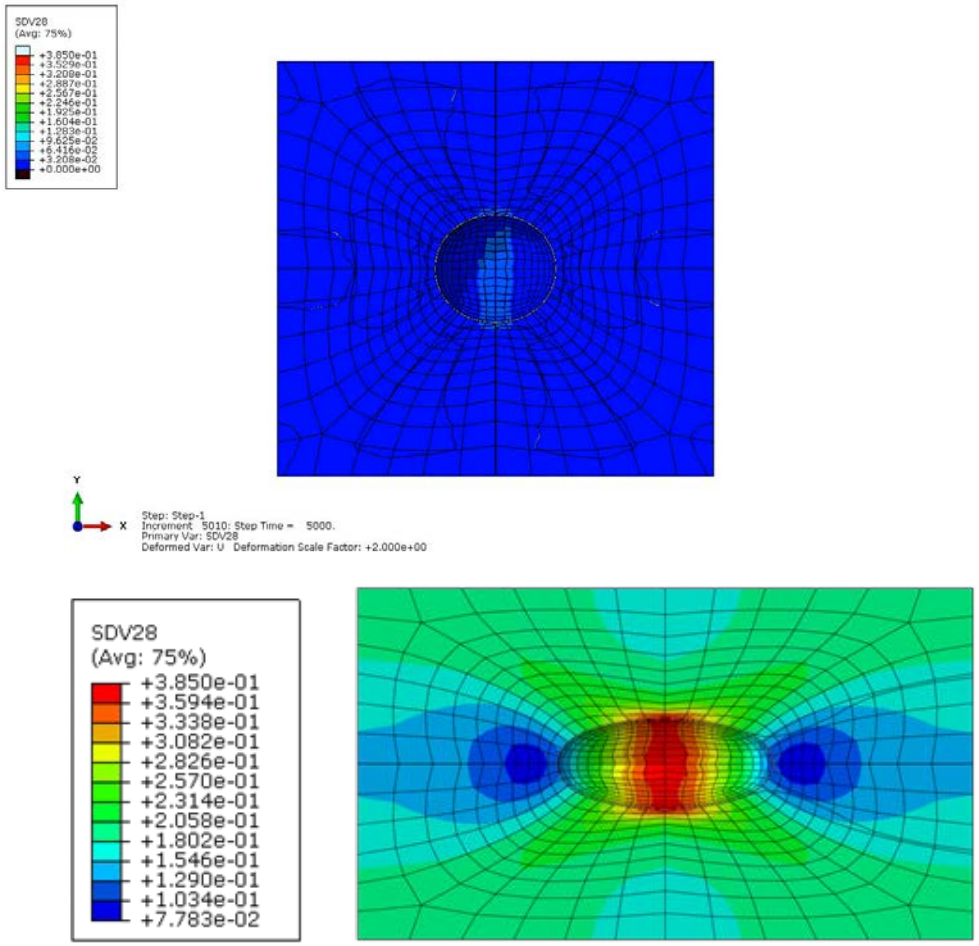

Bicrystal sample (tilt 45º)

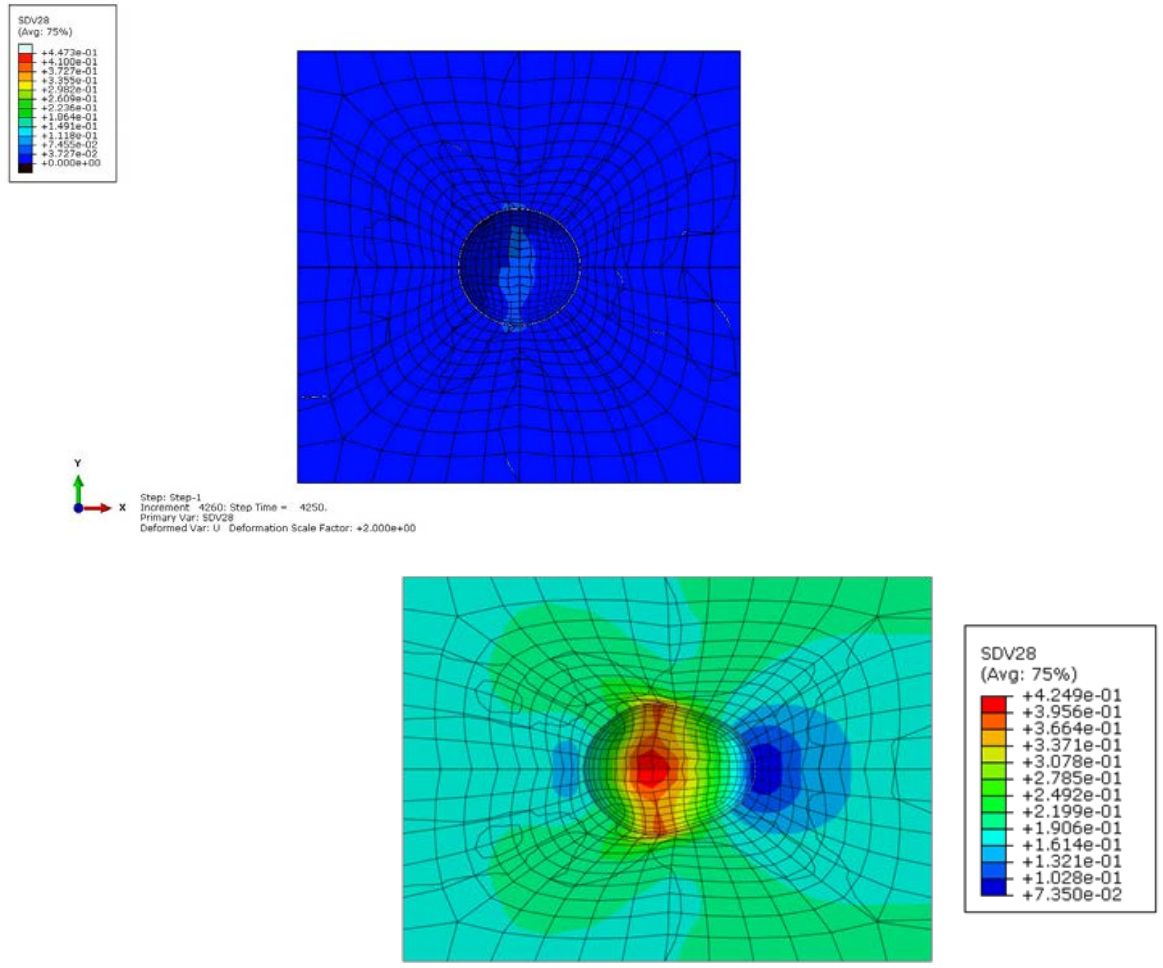

Crystal plasticity finite element method

Void growth on GBs in bicrystal samples

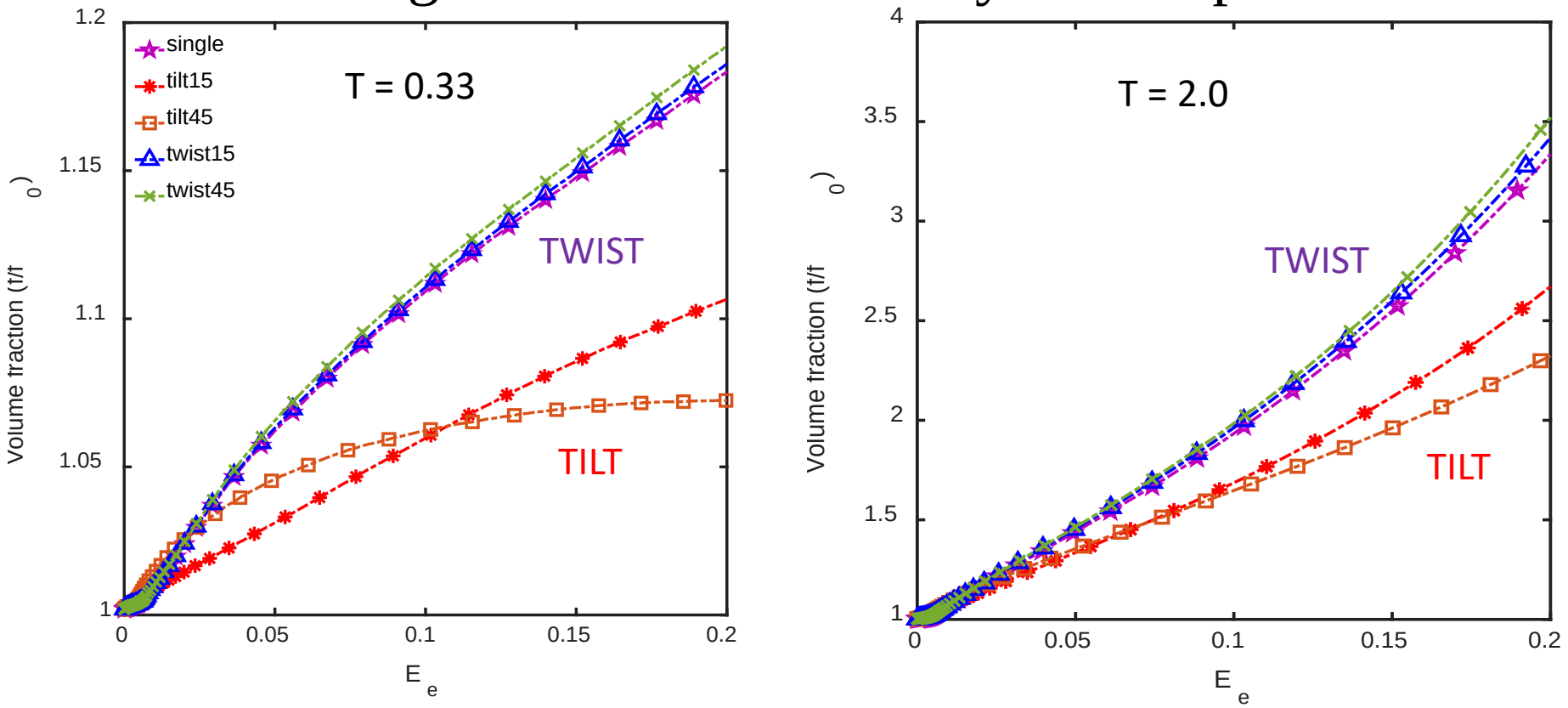

- Higher stress triaxiality induced faster void growth.
- Tilt GBs suppressed the void growth, when the main loading axis was perpendicular to the GB.
- Variation in the twist GBs exhibited little influence on the void growth.

Crystal plasticity finite element method

Effective Schmid factors

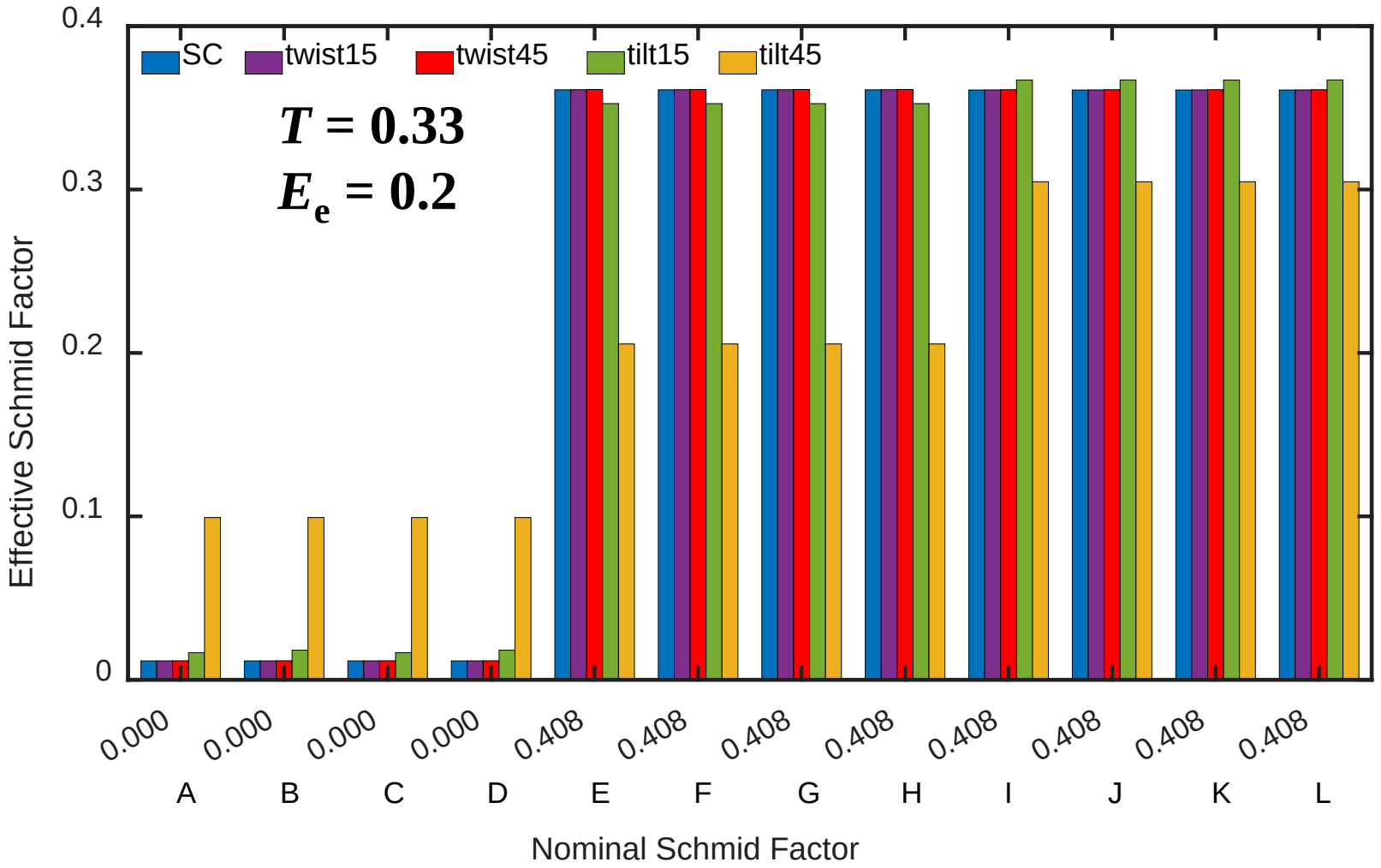

Unbalanced accumulate shear strain is induced by the change of the effective Schmid factors.

Conclusion: Crystal Plasticity Model

1) In both single crystal and crystal samples, the void volume increases with the macro-equivalent, and higher stress triaxiality induced faster void growth.

2) Tilt GBs suppressed the void growth, when the main loading axis was perpendicular to the GB. While variation in twist GBs exhibited little influence on the void growth.

3) Interactions between the two grains bonded to the tilt GBs altered the local stress status in both crystals and ultimately induced the unbalanced accumulate shear strain in the original grains with symmetric slip systems.

Overall conclusions (Q1-Q5)

- We have developed fundamental understanding on the chemical bonding mechanisms and elastic properties
- We have developed new transferable EAM potentials suited for M-C systems → critical components of the precipitate systems at GBs
- We have evaluated the dislocation dynamics as a function of voids and strengthening agent distribution → ported to FEA analysis
- We have systematically assessed void growth dynamics in single and bi-crystal model samples as a function of GB orientations.

Presentations and publications

- Presentations (underlined: undergraduate students):
  - (Invited) Caizhi Zhou, Tianju Chen, Ridwan Sakidja, Wai-Yim Ching, "Effect of the crystallographic orientation on the void growth during creep of superalloys", TMS 2019 Annual Meeting & Exhibition, March 10-14, 2019, San Antonio, Texas.
  - Puja Adhikari, Saro San, CiaZhi Zhou, Rdiwan Sakidja, and Wai-Yim Ching, *First-principles calculation of crystalline precipitate phases $M_{23}C_6$(M = Cr, W, Mo, Fe) in Ni-based supper-alloys, XVI European Ceramic Conference in Torino (Italy) June16-20, 2019.*
  - Wai-Yim Ching and Saro San, Electronic structure and mechanical properties of Ni-based superalloys: Haynes282 and Inconel740, 43rd ICACC, Jan 27-Feb-1 2019, Daytona Beach, FL.
  - Saro San and Wai-Yim Ching, Ab initio modeling of large defects in -Ni and -Ni, 43rd ICACC, Jan 27-Feb-1 2019, Daytona Beach, FL.
  - Austin Bollinger, Ridwan Sakidja, "Molecular Dynamic Simulations of Layered Metallic Systems". Presentations at the Arkansas Idea Networks of Biomedical Research Excellence (INBRE), Nov. 2nd-3rd,2018 at the University of Arkansas in Fayetteville, AR.
  - Tyler McGilvry-James, Nirmal Baishnab, Ridwan Sakidja, "Molecular Dynamics (MD) Potential Development for Carbides". Presentations at the Arkansas Idea Networks of Biomedical Research Excellence (INBRE), Nov. 2nd-3rd,2018 at the University of Arkansas in Fayetteville, AR.
  - Rabbani Muztoba, Nirmal Baishnab, Sabila Kader, Ridwan Sakidja– Development of multi-component EAM potential for Ni-based Superalloys, Presentations at the Materials Science & Technology (MS&T)2018 in Columbus, OH , October 14-18, 2018
  - Sabila Kader Pinky, Muztoba Rabbani, Ridwan Sakidja –Molecular Dynamics Study of Creep Deformation in Nickel-based Superalloys, Presentations at the Materials Science & Technology (MS&T)2018 in Columbus, OH , October 14-18, 2018
- Publications:
  - Tianju Chen; Ridwan Sakidja; Wai-Yim Ching; Caizhi Zhou, “Crystal plasticity modeling of void growth on grain boundaries in Ni-based superalloys“, JOM *(under review).*
  - Puja Adhikari, Saro San, Caizhi Zhou, Ridwan Sakidja, and Wai-Yim Ching, “Electronic structure and mechanical properties of crystalline precipitate phases $M_{23}C_6$ (M = Cr, W, Mo, Fe) in Ni-based superalloy”, Physical Review Materials *(under review)*.

Extended Creep Model on Ni-based Superalloys:

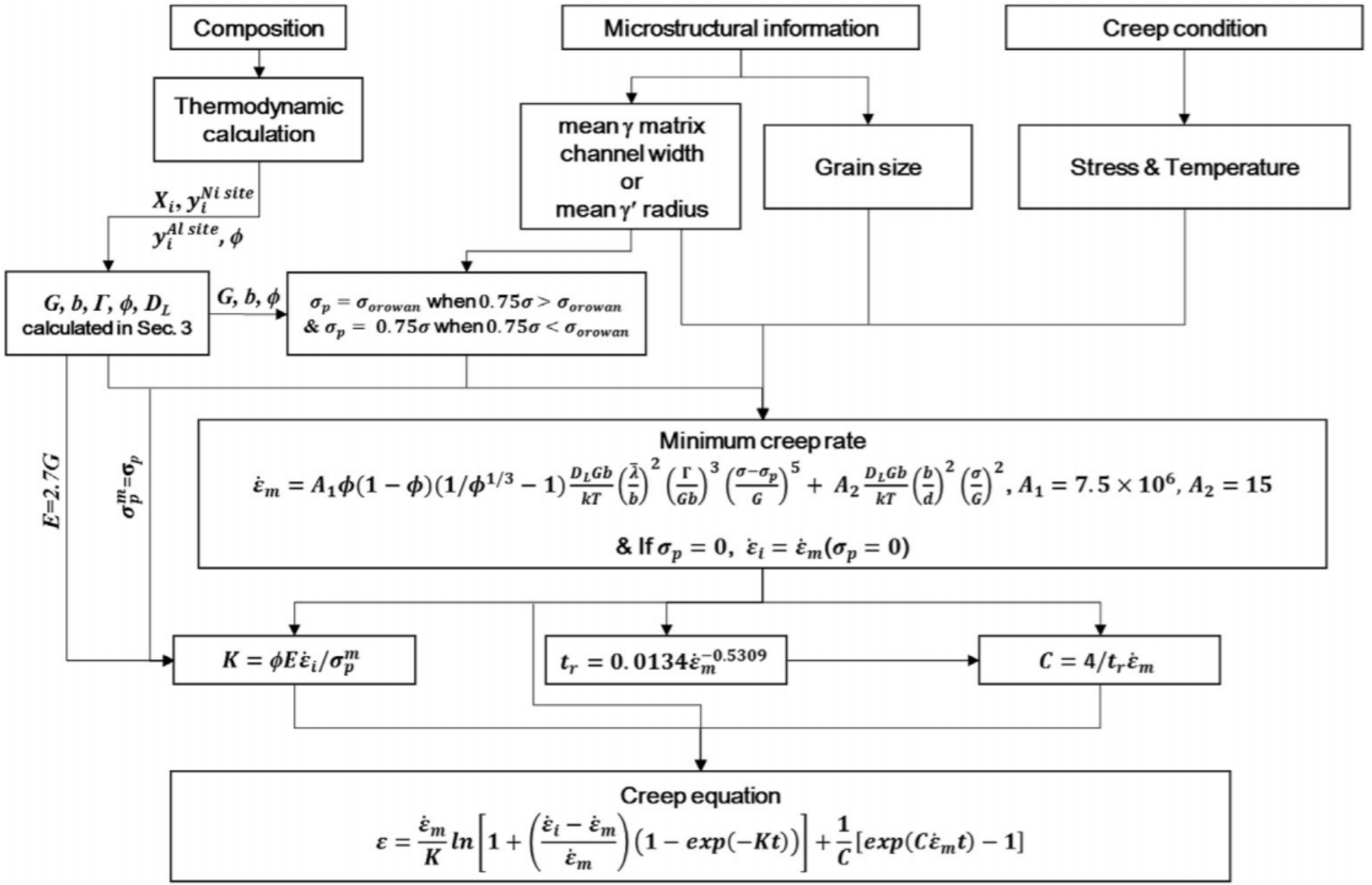

Kim et. al, International Journal of Plasticity 79 (2016) 153-175 (Byeong-Joo Lee's group)

Extended Creep Model on Ni-based Superalloys:

Needs alloy-specific $t_R - \varepsilon'_m$ correlations

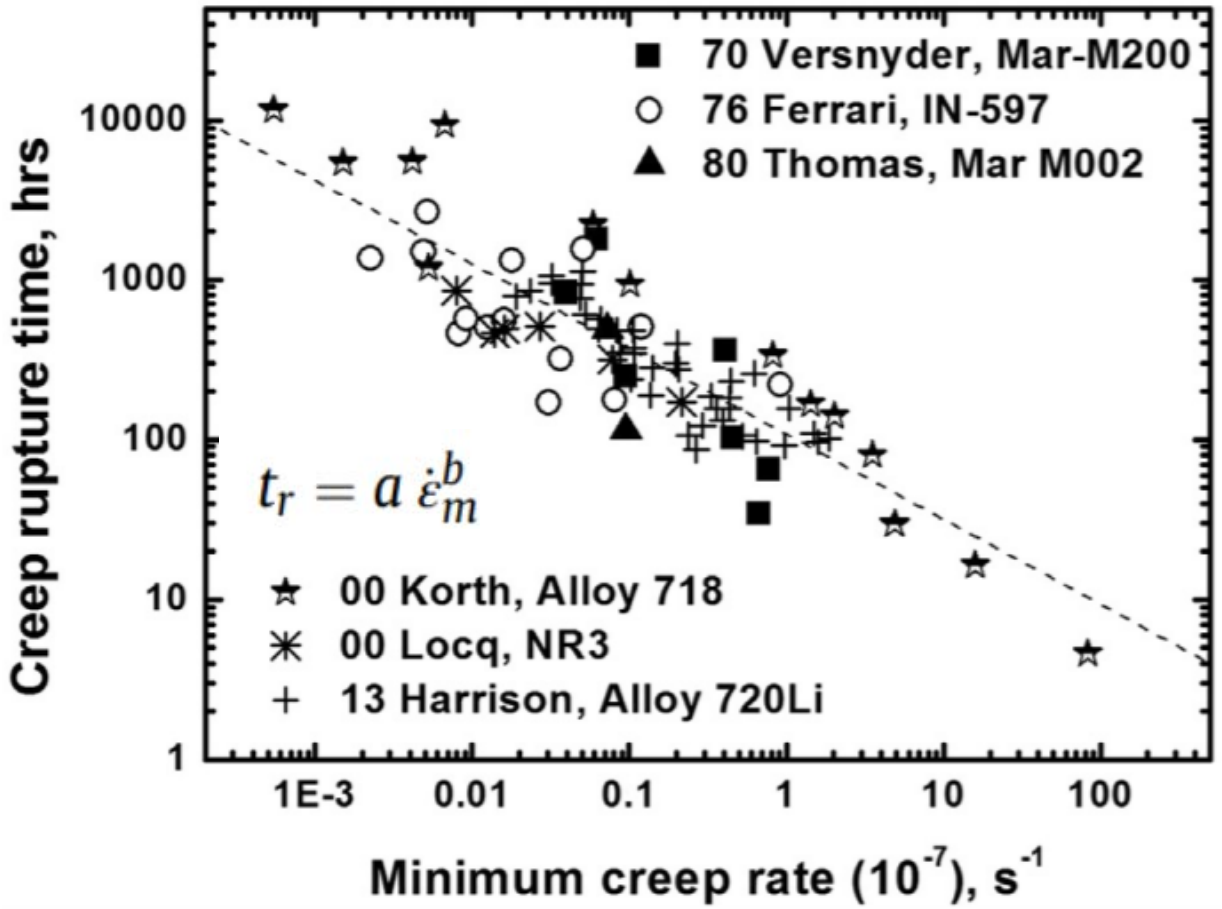

GOOD Prediction
René 88DT

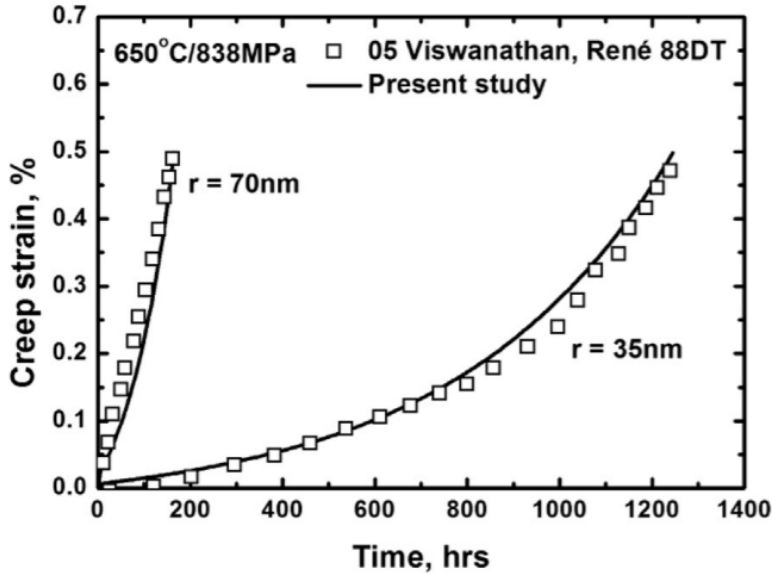

UNDERESTIMATED
for NR3

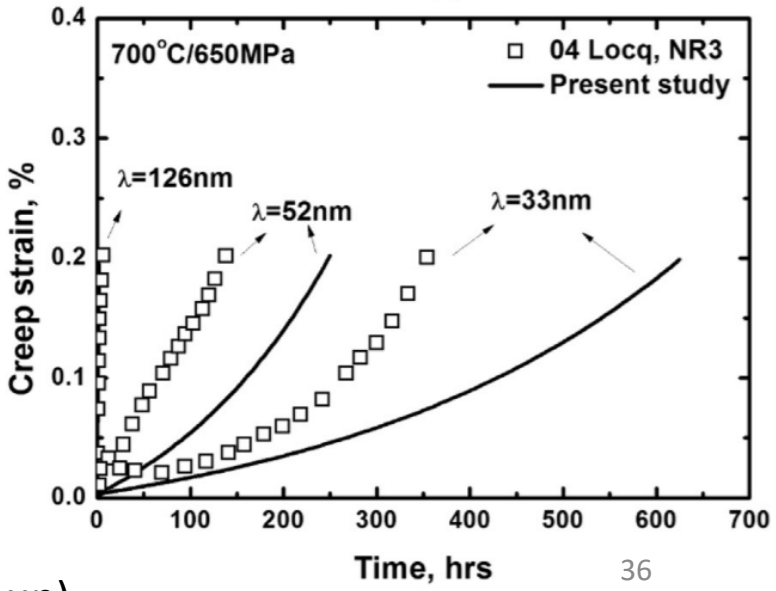

Kim et. al, International Journal of Plasticity 79 (2016) 153-175 (Byeong-Joo Lee's group)